

**RI**

**8544**

**Bureau of Mines Report of Investigations/1981**

**NATIONAL MINE HEALTH & SAFETY ACADEMY  
REFERENCE COPY  
Do Not Remove From Learning Resource Center**

## **Design Parameters for Oil Shale Waste Disposal Systems**

**By R. A. Bloomfield and B. M. Stewart**



**UNITED STATES DEPARTMENT OF THE INTERIOR**



**Report of Investigations 8544**

# **Design Parameters for Oil Shale Waste Disposal Systems**

**By R. A. Bloomfield and B. M. Stewart**



**UNITED STATES DEPARTMENT OF THE INTERIOR**  
**James G. Watt, Secretary**  
**BUREAU OF MINES**

This publication has been cataloged as follows :

**Bloomfield, Roger A**

Design parameters for oil shale waste disposal systems.

(Report of Investigations - Bureau of Mines ; 8544)

Bibliography: p. 35-36.

Supt. of Docs. no.: I 28.23:8544.

I. Oil-shale industry—Waste disposal. I. Stewart, Bill, joint author.  
II. Title. III. Series: United States. Bureau of Mines. Report of investigations ; 8544.

TN23.U43 [TD899.P4] 622s [655'.4] 80-606995

## CONTENTS

	<u>Page</u>
Abstract.....	1
Introduction.....	1
Acknowledgments.....	3
Material properties.....	3
Physical properties.....	4
Engineering properties.....	5
Compaction characteristics.....	5
Consolidation.....	6
Unconfined compression.....	8
Triaxial compression strength.....	9
Direct shear tests.....	10
Permeability.....	11
Cyclic triaxial tests.....	12
Hydraulic properties.....	12
Natural cementation properties.....	13
Field tests and modeling.....	20
Compaction tests.....	20
Seepage ponds.....	24
Preliminary disposal systems.....	27
Underground disposal.....	27
Surface disposal.....	30
Stability analysis.....	31
Conclusions.....	33
References.....	35
Appendix.--Nomenclature.....	37

## ILLUSTRATIONS

1. Gradation ranges of Paraho and Tosco retorted oil shale.....	4
2. Effect of curing time on the unconfined compressive strengths of Paraho and Tosco retorted oil shale.....	8
3. Failure envelopes for direct shear tests on Paraho retorted oil shale.....	10
4. Permeability-void ratio relationships for compacted Paraho and Tosco retorted oil shale.....	11
5. Cyclic triaxial response of compacted Paraho retorted oil shale....	12
6. Comparison of capillary pressure-saturation data from undisturbed cores and from laboratory-packed samples.....	13
7. Relative conductivity-capillary pressure curves from undisturbed cores of Paraho compacted retorted oil shale.....	14
8. Seven-day compressive strength of retorted oil shale after addition of moisture, compaction, and curing at 100° F.....	17
9. Fifteen-day compressive strength of retorted oil shale after addition of moisture, compaction, and curing at 100° F.....	17
10. Twenty-eight-day compressive strength of retorted oil shale after addition of moisture, compaction, and curing at 100° F.....	18
11. Forty-day compressive strength of retorted oil shale after addition of moisture, compaction, and curing at 100° F.....	18

## ILLUSTRATIONS--Continued

	<u>Page</u>
12. Retorted oil shale fragment with clumps of crystals (X 115).....	19
13. Gradation curves of fill material before and after compaction and of material directly from the retort.....	22
14. Comparison of actual and simulated flow of water through pond 2 constructed of loose-packed Paraho retorted oil shale.....	25
15. Typical cross-valley fill and simulated saturation zone after 1 year of ponding.....	31
16. Circular arc failure planes and safety factors for a saturated and dry retorted oil shale fill.....	32
17. Circular arc failure plane and safety factor for a saturated retorted oil shale fill with a core.....	33

## TABLES

1. Summary of compaction characteristics for Paraho and Tosco oil shale.....	5
2. Consolidation parameters for Paraho and Tosco retorted oil shale at maximum applied stress.....	7
3. Summary of total and effective strength parameters for Paraho and Tosco.....	9
4. Simulation of commercial retorting conditions.....	15
5. Summary of test fill compaction data.....	21
6. Boundary conditions and values of parameters for simulation of pond 2.....	26
7. Cumulative leaching after sprinkling.....	27
8. Ranking analysis final selection for chamber-and-pillar mining.....	28
9. Ranking analysis final selection for sublevel stoping.....	29

# DESIGN PARAMETERS FOR OIL SHALE WASTE DISPOSAL SYSTEMS

by

R. A. Bloomfield<sup>1</sup> and B. M. Stewart<sup>2</sup>

---

---

## ABSTRACT

This report summarizes Bureau of Mines contract research on the disposal of retorted oil shale. A data base has been developed describing the physical-chemical properties, geotechnical engineering properties, and natural cementation characteristics of spent shale. Results of field compaction tests and seepage pond tests are presented, along with results of a partially saturated finite element seepage model used to predict infiltration and seepage rates. Preliminary engineering analyses are presented for underground disposal systems, which include material transport methods, and for a surface disposal system, which includes stability analyses.

## INTRODUCTION

A major problem area in considering commercial oil shale operations is the efficient disposal of the spent shale in a structurally and environmentally safe manner. In surface retorting operations, the spent shale occupies about a 20 percent greater volume than in-place raw shale. Therefore, whether the mining operation is open pit or underground, some surface disposal will be required even if backfilling is employed. If modified in situ retorting techniques are utilized, a surface disposal problem is still present, since raw shale is excavated when developing the underground retorts.

In order to construct efficient waste management systems and comply with environmental restrictions, a thorough knowledge of the physical-chemical and engineering properties of shale waste is required. This report is intended to summarize in-house Bureau of Mines research and Bureau-funded contract research relating to spent shale disposal techniques. The following contracts were funded by the Bureau of Mines over the past 5 years.

1. "Disposal of Retorted Oil Shale From the Paraho Oil Shale Project"  
(5)<sup>3</sup>--This project included both field and laboratory testing of the

---

<sup>1</sup>Program manager, Division of Minerals Environmental Technology, Bureau of Mines, Washington, D.C.

<sup>2</sup>General engineer, Spokane Research Center, Bureau of Mines, Spokane, Wash.

<sup>3</sup>Underlined numbers in parentheses refer to items in the list of references preceding the appendix.

engineering properties of spent shale. The Paraho process produces waste material with a maximum particle size of about 3 inches in diameter and ranging down to 10 to 30 percent passing a No. 200 sieve. If a high compactive effort is used, the material can be compacted to over 100 pounds per cubic foot (pcf), which results in good strength characteristics and is semipervious to impervious. At low compactive efforts, the spent shale is very permeable, similar to a silty gravel. Permeability tests were performed on field test ponds. In a simulated rainfall test of 2 inches in 30 minutes, which required 4,600 gallons of water, only 2 gallons permeated through the 3.5-foot-deep test area. No water had been ponded on this test section for the previous 3-1/2 months, so some of the water from the simulated rainfall test was absorbed and adsorbed by the spent shale particles. Field tests also showed that the spent shale did not exhibit autoignition tendencies when spread over test fills.

2. "Seepage Through Partially Saturated Shale Waste" (2)--Oil shale waste disposal systems are likely to remain in a partially saturated condition, because of the semiarid climate and lack of excess water. An existing finite-element computer code was modified and tested to handle seepage problems expected in partially saturated waste disposal systems. Hydraulic properties of the shale waste were determined in the laboratory, and the program was verified by comparing analytical results to laboratory and field tests. Very good correlation was found between computer results and measured seepage from the field filtration ponds tested under the Development Engineering Inc. project (5). This program should be used to predict and analyze seepage patterns when designing a spent shale waste disposal system.

3. "Geotechnical Properties of Oil Shale Retorted by the Paraho and Tosco Processes" (10)--The objective of this project was to obtain a complete and detailed compilation of engineering properties for both Paraho and Tosco shale waste. This comprises the largest set of data available, and results from the other shale waste contracts will serve as supplemental and comparative data. Properties determined included specific gravity, compaction, consolidation, unconfined and triaxial compressive strength, direct shear strength, cyclic shear strength, resonant column, and permeability tests. Results of this project provide a complete and detailed set of engineering design parameters, which are necessary for the design of full-scale disposal systems.

4. "Underground Disposal of Retorted Oil Shale for the Paraho Retorting Process" (3)--The objective of this contract was to determine the most desirable systems for underground disposal of retorted oil shale from the Paraho process, based on chamber-and-pillar and sublevel stoping mining methods. The backfilling methods studied were hydraulic, pneumatic, and mechanical, both alone and in combination. Conveyor transport was found to be most feasible. Indications are that 70 to 85 pct of the retorted shale can be returned to the mine. Underground backfilling can reduce the surface environmental impact of retorted shale disposal by cutting back on the land needed for total disposal. Industry can use study results in future planning of large-scale underground oil-shale mining.

5. "Natural Cementation of Retorted Oil Shale" (4)--This project included an extensive laboratory program studying the relationship of retort conditions on waste sample strength. The objectives were to (1) determine optimum retort time and temperature required to develop maximum natural cemented strength in samples; (2) determine the natural cementation constituents; (3) determine the effects on density, permeability, and leachate quality for different retort conditions; and (4) determine the effect of reusing retort water on strength and leachate quality. These results will be useful in evaluating the long-term stability of shale waste systems.

#### ACKNOWLEDGMENTS

The authors wish to express their gratitude to Howard Earnest, Rio Blanco Oil Shale Co. (formerly with Cleveland-Cliffs Iron Co.); George Bloomsburg, University of Idaho; Wes Holtz, Woodward-Clyde Consultants; Frank Townsend, University of Florida (formerly with Waterways Experiment Station, U.S. Army Corps of Engineers); and Clifford Farris, Council of Energy Resource Tribes (formerly with Colorado School of Mines Research Institute). Without the hard work, cooperation, and dedication of these principal investigators, the physical properties needed for design of oil shale waste disposal systems could not have been reported. The five Bureau of Mines open file reports, from which data for this report were obtained, were excellently written by these five men and exhibited a high degree of engineering expertise.

The authors also thank John Jones, Jr., and Phil Trumbo, Development Engineering Inc.; Mark Atwood, Tosco; R. A. Heisler, H. L. Hoe, and V. Rajaram, Cleveland-Cliffs Iron Co.; Dick Peterson, Waterways Experiment Station; and R. D. Wells, University of Idaho. These men were highly instrumental in the successful completion of the five Bureau research projects used for this report.

#### MATERIAL PROPERTIES

Spent shale used in determining the physical, chemical, and engineering properties was retorted by the Paraho and Tosco processes as noted in this report. The Paraho process produces a coarser waste with a maximum particle size of about 3-inch (7.6-cm) diameter, while the Tosco material has a maximum size of about 1/2-inch (1.27-cm) diameter. Shale used in determining the natural cementation characteristics was retorted in the laboratory where closer control of retort temperature and residence time could be maintained.

Wherever possible, a range of values is presented when describing material properties. These results are intended to be used as a guideline in developing preliminary designs. Before any detailed design work is performed, a small-scale laboratory testing program is necessary using material from the appropriate retorting technique processed at the anticipated retorting conditions. Changes in retort temperature and residence time will alter the properties to some extent, which is one reason why a range of values is presented here. In addition, the tests were performed in five different engineering laboratories utilizing procedures as outlined by the American Society for Testing and Materials (1), U.S. Army Corps of Engineers (11), and the U.S. Bureau of Reclamation (12).

## PHYSICAL PROPERTIES

The physical property testing consisted of determining the gradation curves, Atterberg limits, and specific gravity. The gradation curves for both Paraho and Tosco spent shale used in these studies are shown in figure 1. The range of values for the Tosco material is very close, showing little variability in the samples tested. There is a wider range with the Paraho material, especially in the finer gradations. A difference in mechanical and hand sieving accounted for a part of this wide range, but most is attributed to experimental crushing operations of the retort feed that were taking place during the time when bulk samples of retorted material were obtained.

Results of Atterberg limits tests showed that the spent shale is non-plastic. The plasticity index ranged from 3 to 5 pct for Paraho and from 5 to 6 pct for Tosco. Using the Unified Soil Classification System, Paraho classifies as a poorly graded sandy gravel (GP), and Tosco classifies as a silty sand (SM). The apparent specific gravity ranged from 2.52 to 2.59 for Paraho and from 2.53 to 2.55 for Tosco.

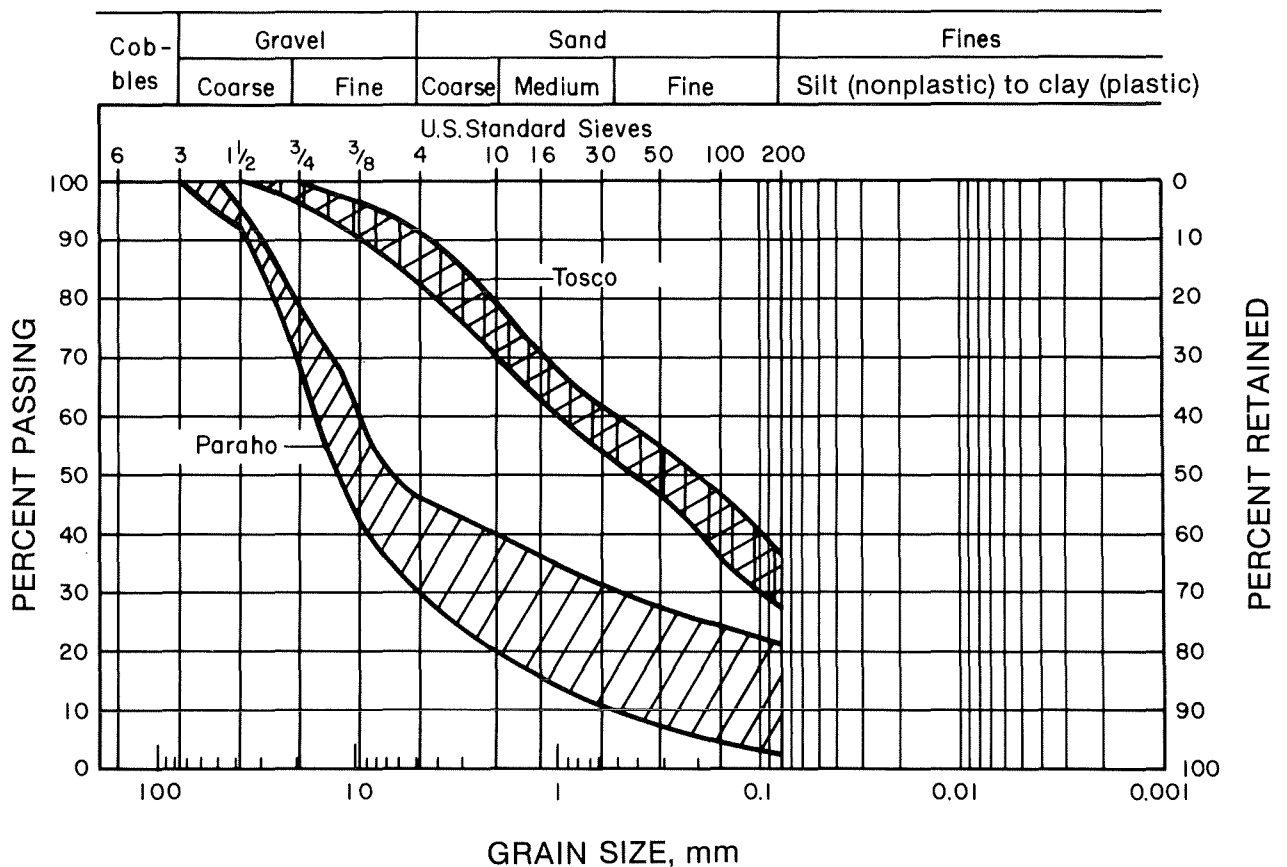


FIGURE 1. - Gradation ranges of Paraho and Tosco retorted oil shale.

## ENGINEERING PROPERTIES

The most comprehensive laboratory determination of engineering properties for both Paraho and Tosco spent shale was performed at the Waterways Experiment Station (10). Much of this section is taken from their report.

Compaction Characteristics

The results of full-scale (12-inch-diameter) (30.5-cm) compaction tests on Paraho and conventional (6-inch-diameter) (15.2-cm) tests on Tosco and modeled (scalped and replaced) Paraho using three compactive efforts, 60 pct of standard (60 pct std) Proctor, standard Proctor, and modified Proctor compactive efforts, are presented in table 1.

TABLE 1. - Summary of compaction characteristics for Paraho and Tosco oil shale

Compaction effort	Maximum dry density, d, pcf	Minimum dry density, d, pcf	Water content, W, pct	Breakage factor, B, pct
PARAHO (MINUS 2-INCH MATERIAL)				
Vibratory.....	89.2	66.0	-	-
60 pct std Proctor.....	94.6	-	23.3	11
Do.....	92.5	-	0	-
Standard Proctor.....	97.5	-	22.2	16
Do.....	96.3	-	0	-
Modified Proctor.....	104.4	-	18.4	25
Do.....	103.9	-	0	-
MODELED PARAHO (MINUS 3/4-INCH MATERIAL)				
Vibratory.....	81.8	62.9	-	-
60 pct std Proctor.....	91.9	-	27.2	20
Do.....	85.6	-	0	-
Standard Proctor.....	95.7	-	25.3	24
Do.....	90.0	-	0	-
Modified Proctor.....	103.1	-	17.7	34
Do.....	100.0	-	0	-
TOSCO (MINUS 1-INCH MATERIAL)				
60 pct std Proctor.....	97.0	-	21	-
Standard Proctor.....	99.0	-	19	-
Modified Proctor.....	104.0	-	18	-

In the case of both full-scale and modeled Paraho, to achieve the maximum dry density, sufficient water to practically saturate the material is required. However, for the full-scale material, water contents less than optimum produced bulking and the difference between maximum dry density at optimum and the dry condition is small (as shown in table 1). This indicates that compaction of Paraho in the retorted condition is feasible. An alternative to using water to increase density is obviously to increase the compaction effort. It is important to observe that this conclusion would not have been reached using results of smaller compaction tests and modeled material. For the modeled material, compaction in the dry condition produced densities considerably lower than those at optimum water contents.

Table 1 also presents the breakage factor, B, which is the sum of the differences in percent retained on each sieve before and after compaction, with greater breakage occurring with increased compactive effort.

The results also show that particles of the finer modeled gradation experienced greater breakage than did those of the coarser full-scale gradation, which is contrary to expectations; for example, coarser particles generally experienced a greater amount of particle breakage. One possible explanation for this anomaly is that the impact energy per compaction foot-area delivered by the hand-held rammer used with the 6-inch-diameter (15.2-cm) mold is considerably (3 times) greater than that for the 12-inch-diameter (30.4-cm) mold.

The compaction test results using three compactive efforts on Tosco are also summarized in table 1. Quite unlike the full-scale Paraho, the effect of water content on Tosco was to produce increasing densities until optimum was achieved. Thus, the economics of adding water for compaction or increasing compactive effort to achieve a specified density is much more critical.

Results listed in table 1 show that the maximum dry density achieved by vibration was considerably lower than the maximum achieved by only 60 pct std effort. It might be concluded that Paraho does not respond favorably to laboratory compaction using the vibratory method. Nevertheless, field compaction tests (5) showed that a vibrating drum roller provided the best compaction of Paraho.

#### Consolidation

Table 2 summarizes the results of 12-inch-diameter (30.5-cm) consolidation tests on Paraho and Tosco to a maximum vertical stress of 800 psi (5.52 mpa) for samples that were densified by three different compactive efforts. These results show the expected trend of decreasing vertical strain, coefficient of compressibility, and permeability with increased compactive effort. The  $10^{-7}$  cm/sec permeability values for both Paraho and Tosco indicate that these materials will be relatively impervious when compacted and subjected to high stresses. This low value of permeability for the Paraho material was unexpected considering the small percentage of fines. The breakage factor, B, values presented in table 2 are a composite of breakage suffered during specimen compaction and application of vertical stresses during consolidation. Breakage values during compaction listed in table 1 for Paraho were 11 and 16 pct, respectively, for 60 pct std and standard compactive efforts.

TABLE 2. - Consolidation parameters for Paraho and Tosco retorted oil shale  
at maximum applied stress (800 psi) (10)

Material and compactive effort	Vertical <sup>1</sup> strain, pct	Coefficient of compressibility, $A_v = \Delta e / \Delta P$ , cm <sup>2</sup> /kg	Compression index, $C_c = \Delta e / \log P_2/P_1$ , cm <sup>2</sup> /kg	Coefficient of consolidation, $C_v = \frac{0.848H^2}{t_{90}}$ , cm <sup>2</sup> /sec	Permeability, $k = \frac{C_v A_v Y_w}{1 + e}$ , cm/sec	Breakage <sup>2</sup> factor, B, pct
Paraho:						
60 pct std..	10.0	0.0021	0.1495	0.293	$4.2 \times 10^{-7}$	27
Standard....	7.7	.0015	.1080	.442	$4.7 \times 10^{-7}$	27
Modified....	4.7	.0010	.0963	.433	$3.1 \times 10^{-7}$	
Tosco:						
60 pct std..	8.4	.0014	.0963	.358	$3.2 \times 10^{-7}$	44
Standard....	6.7	.0014	.1262	.451	$4.0 \times 10^{-7}$	29
Modified....	4.7	.0011	.0996	.352	$2.5 \times 10^{-7}$	

$${}^1 E = \frac{\Delta e}{1 + e_0} = \frac{e_0 - e_{800}}{1 + e_0}$$

<sup>2</sup>Combined compaction and consolidation.

NOTE.--Ft/yr =  $0.97 \times 10^{-6}$  cm/sec.

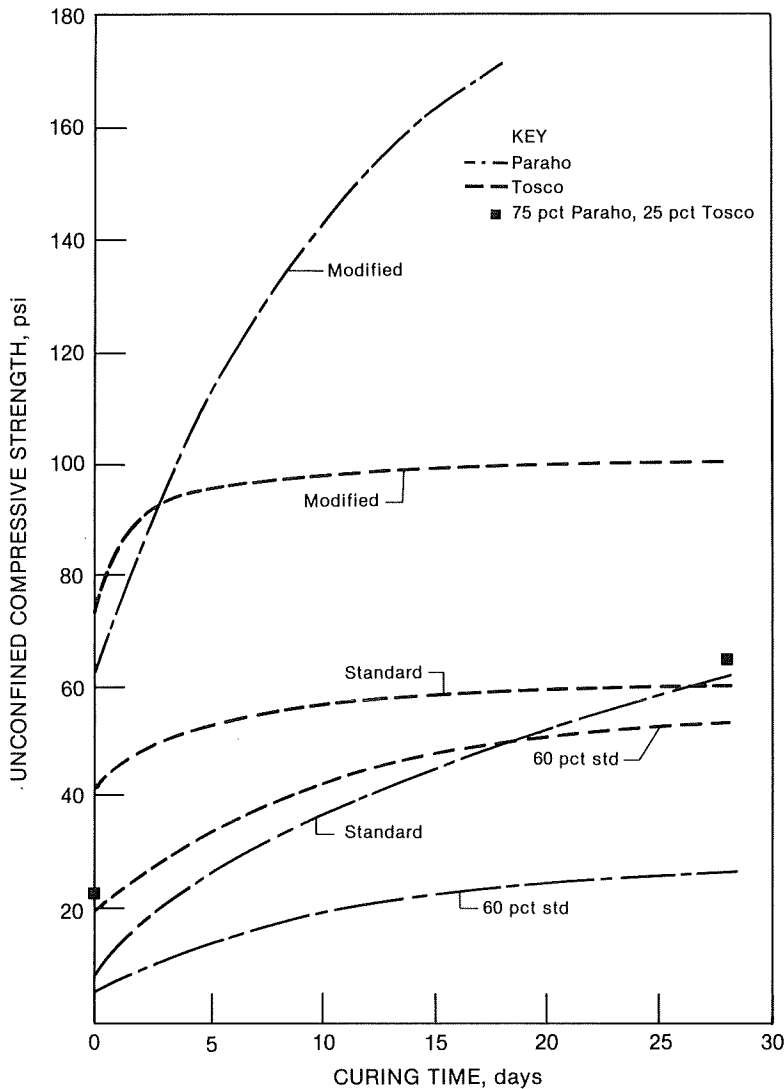


FIGURE 2. - Effect of curing time on the unconfined compressive strengths of Paraho and Tosco reorted oil shale.

nature of the Tosco permits cementation reactions to be completed more rapidly than the coarser Paraho material.

The data presented in figure 2 also reveal that Paraho is more reactive than Tosco. Tosco initial strengths are higher than corresponding Paraho initial strengths. The Paraho specimens, except at 60 pct std effort, exhibit higher strengths after 28 days' curing. While it might be anticipated that the finer nature of Tosco would be more reactive, the results did not confirm the theory. Perhaps the fine-grained nature of Tosco makes the self-cementing components susceptible to deterioration upon prolonged exposure, while coarser grained Paraho breaks down more during compaction and exposes fresh surfaces for reaction. If this is the case, then delay between retorting and fill placement becomes an important construction variable.

### Unconfined Compression

To investigate self-cementing characteristics of oil shale waste, 6-inch-diameter (15-cm) unconfined compression (U/C) tests were performed on a number of specimens, which were compacted using three different compactive efforts and allowed to cure at ambient temperatures for periods ranging from 0 to 28 days. Figure 2 summarizes the effects of curing time on U/C strength, and shows that the strength increases with age, a characteristic indicative of self-cementing. The magnitude of cementation is dependent upon time and density, and increases proportionally with these variables. The durability of several specimens was examined by soaking overnight, and no strength loss was observed.

A comparison between Paraho and Tosco shows that Paraho reacts more slowly than Tosco and continues to gain strength beyond 28 days. Conversely, Tosco appears to gain most of its strength within 3 days after compaction. Perhaps the finer

Also included in figure 2 are the results of 0- and 28-day tests on specimens using a 75-pct Paraho and 25-pct Tosco mixture.

### Triaxial Compression Strength

Strength parameters for the three compactive efforts were determined by performing a series of consolidated-drained (CD), or consolidated-undrained (CU), triaxial compression tests with pore pressure measurements on 9-inch-diameter (22.9-cm) specimens of Paraho material. Supplementary CU tests were performed on 6-inch-diameter (15.2-cm) and 1.4-inch-diameter (3.6-cm) specimens of modeled Paraho and Paraho fines, respectively, prepared at equivalent standard effort density. A series of CU tests on 6-inch-diameter (15.2-cm) specimens of Tosco compacted to three different densities were used to determine the strength of this material.

Table 3 summarizes the total and effective strength parameters for Paraho and Tosco. A comparison of these results for Paraho show that except for a higher cohesion intercept (c), increased compactive effort from 60 pct std to standard effort does not noticeably improve strength. Similarly for Tosco, little strength improvement is observed by increasing the compactive effort from 60 pct std to standard effort. Modified compactive effort is required to significantly increase strength. The effects of modeling on the strength of Paraho are also presented in table 3. A comparison of these results indicated that modeling unconservatively overestimates the effective angle of internal friction ( $\phi'$ ) by  $5.3^\circ$  and the cohesion intercept by  $0.3 \text{ kg/cm}^2$  for standard effort density specimens.

TABLE 3. - Summary of total and effective strength parameters for Paraho and Tosco

Material and compaction effort	Maximum particle size, inches	Total stress		Effective stress	
		$\phi$ , deg	c, $\text{kg/cm}^2$	$\phi'$ , deg	c', $\text{kg/cm}^2$
Full-scale Paraho, 9-inch-diam:					
60 pct std.....	1-1/2			33.0	0.9
Standard.....	1-1/2	14.5	1.3	32.7	.8
Modified.....	1-1/2	<sup>1</sup> 31.0	0	32.3	1.9
Modeled Paraho:					
9-inch-diam, standard <sup>1</sup> ....	3/4			38.0	0
6-inch-diam, standard.....	3/4	17.1	1.7	37.9	1.1
Paraho fines, 1/4-inch-diam, standard.....	1/4	23.2	1.7	33.6	2.3
Tosco, 6-inch-diam:					
60 pct std.....	3/4	20.2	.3	36.7	.1
Standard.....	3/4	18.4	.3	35.0	.1
Modified.....	3/4	24.5	1.4	43	0

<sup>1</sup>Based upon single test.

### Direct Shear Tests

The results of multistaged, consolidated-drained (CD) direct shear tests on dry and inundated 2- by 2- by 1-foot (0.6-m by 0.6-m by 0.3-m) specimens of full-scale Paraho material statically compacted to equivalent standard effort density are presented in figure 3. Comparison direct shear tests on 3- by 3-inch (7.6-cm by 7.6-cm) specimens of modeled Paraho material compacted to equivalent standard effort density are also presented in figure 3. These results show that the failure envelope is curved, and selection of the angle of internal friction is quite dependent upon normal stress. The results also show that inundation causes a reduction in strength for full-scale Paraho material. Also presented in figure 3 is the shear envelope for 9-inch-diameter (22.9-cm) triaxial compression tests on Paraho. A comparison of these results with those for the inundated direct shear tests indicates a reasonable agreement.

The angles of internal friction for CD direct shear tests on 3- by 3-inch (7.6-cm by 7.6-cm) dry and inundated specimens of Tosco material compacted to standard effort density and sheared under a maximum normal stress of 14 kg/cm<sup>2</sup> were 36° and 34°, respectively. These results also indicate that inundation causes a decrease in shear strength. For these tests, the failure envelopes were linear, and no reduction in friction angle with increasing normal stress was observed.

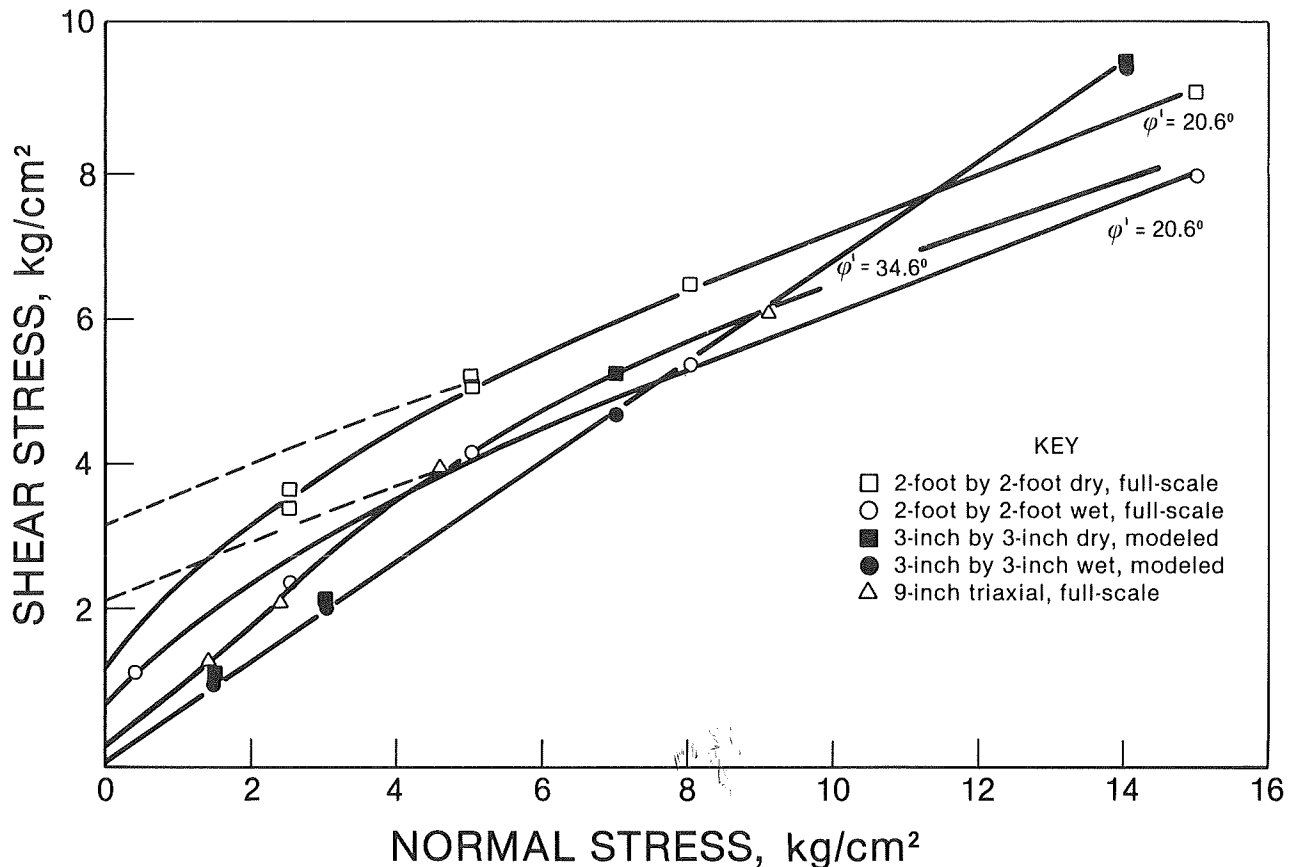


FIGURE 3. - Failure envelopes for direct shear tests on Paraho retorted oil shale.

### Permeability

Figure 4 presents the results of permeability measurements preceding shear of triaxial compression tests on Paraho and Tosco specimens compacted to densities comparable to 60 pct std, standard, and modified compactive efforts. For comparison, permeability values based upon calculations using consolidation data presented in table 2 are also presented. Both sets of data are consistent and show decreasing permeabilities with decreasing void ratios. Generally, the permeabilities for Paraho decrease from  $10^{-3}$  cm/sec for 60 pct std effort densities to  $10^{-4}$  cm/sec for modified effort densities and to  $5 \times 10^{-7}$  cm/sec under an 800-psi load (10). In the case of Tosco, the permeability decreased from  $10^{-6}$  cm/sec to  $10^{-7}$  cm/sec as the compactive effort increased from 60 pct std to modified effort. The permeabilities determined from consolidation tests reflect lower values because of the lower void ratios achieved from higher consolidation stresses.

Generally, materials are classified as impervious if they exhibit permeability values less than  $10^{-6}$  cm/sec, and as pervious if they exhibit permeability values greater than  $10^{-4}$  cm/sec. Hence, depending upon compactive effort, Paraho can be considered as semipervious to impervious, while in the case of Tosco only modified effort compaction will produce an impervious material.

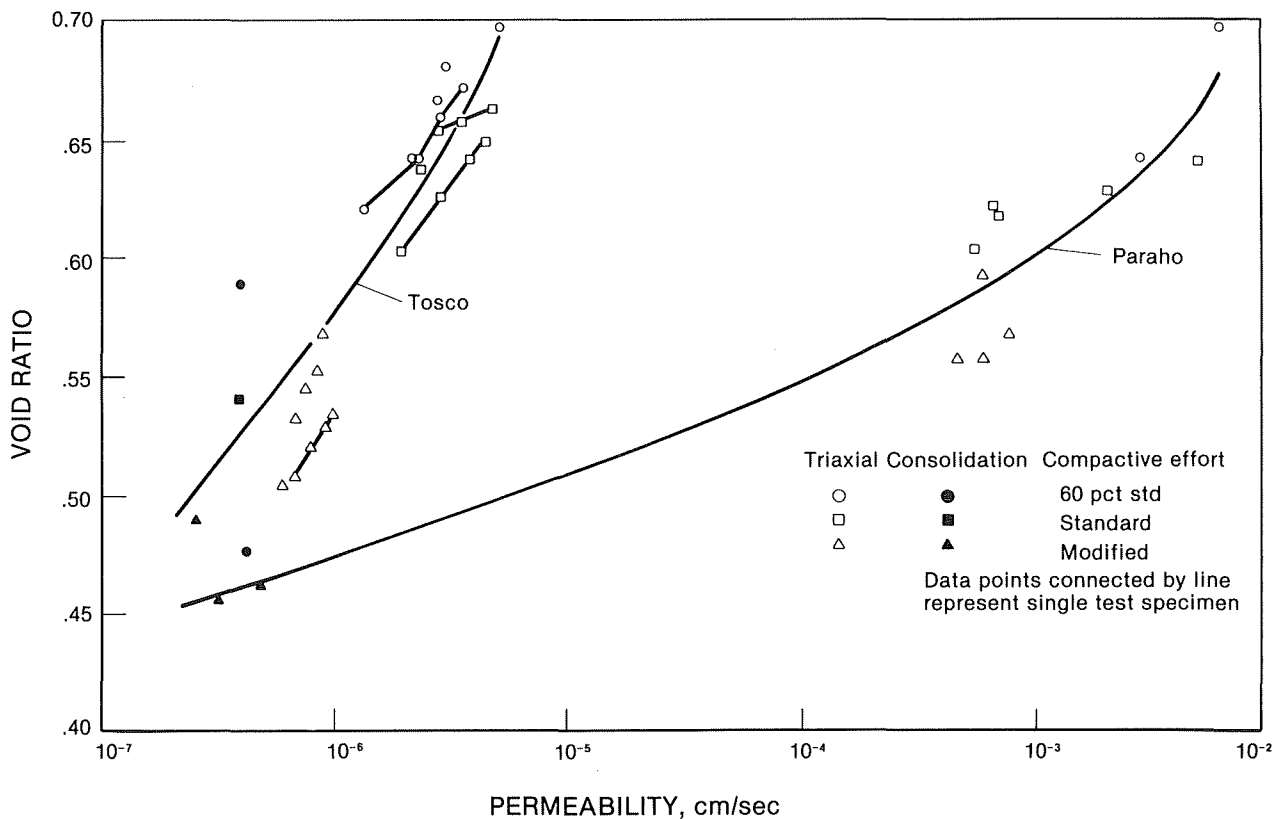


FIGURE 4. - Permeability-void ratio relationships for compacted Paraho and Tosco retorted oil shale.

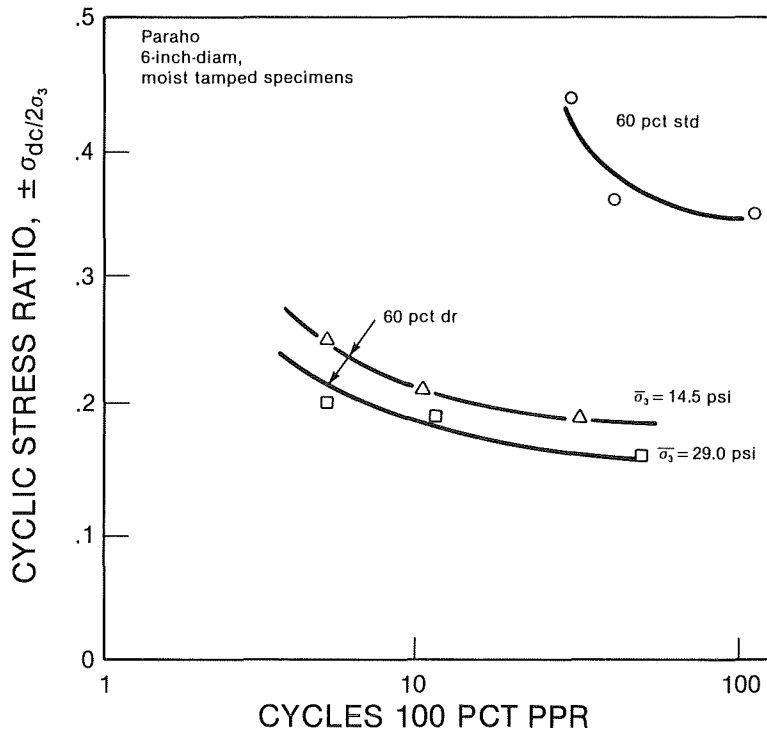


FIGURE 5. - Cyclic triaxial response of compacted Paraho retorted oil shale.

### Cyclic Triaxial Tests

The results of cyclic triaxial tests to assess the resistance of compacted modeled Paraho to seismic forces are presented in figure 5. The first test series was performed on specimens compacted to 60 pct std effort density, and these results show that even at this low compactive effort, the material is quite resistant to cyclic loading. Hence, succeeding tests were performed on moist, tamped specimens compacted to 60 pct relative density (dr). These results show that at this abnormally low density for field conditions, cyclic loading could be a problem. For example, a stress ratio of 0.39 causes 100 pct pore pressure response (PPR) in 10 loading-

unloading cycles for Monterey No. 0 sand moist tamped to 60 pct dr (9), while a stress ratio of only 0.21 resulted in 100-pct PPR for modeled Paraho. The results also show that the cyclic stress ratio ( $\pm\sigma_{dc}/2\sigma_3$ ) required to cause 100-pct PPR decreases with increasing confining pressure, but the practical effect is small.

For comparison, Wung (13) has shown that a cyclic stress ratio of 0.29 was required to cause 5-pct double amplitude strain in 30 cycles for various soils with a mean grain size (D50) similar to modeled Paraho at 60 pct dr. Figure 5 indicates that a cyclic stress ratio of only 0.16 would be required for comparable conditions. From this standpoint, the modeled Paraho at 60 pct dr appears to be weaker than similarly graded materials. Nevertheless, seismically induced ground failure of a waste embankment is deemed an unlikely event, as 100-pct saturation will probably never occur, nor will the materials be deposited in such a loose condition.

### Hydraulic Properties

The computer code used by Bloomsburg (2) to determine unsteady, unsaturated flow characteristics of water through retorted oil shale required the determination of retorted oil shale hydraulic properties as input data. The hydraulic properties include saturated hydraulic conductivity (coefficient of permeability), porosity, and the relationship between capillary pressure ( $P_c/\rho g$ ), saturation (moisture content), and relative conductivity for each material through which water will flow. The saturated hydraulic conductivity

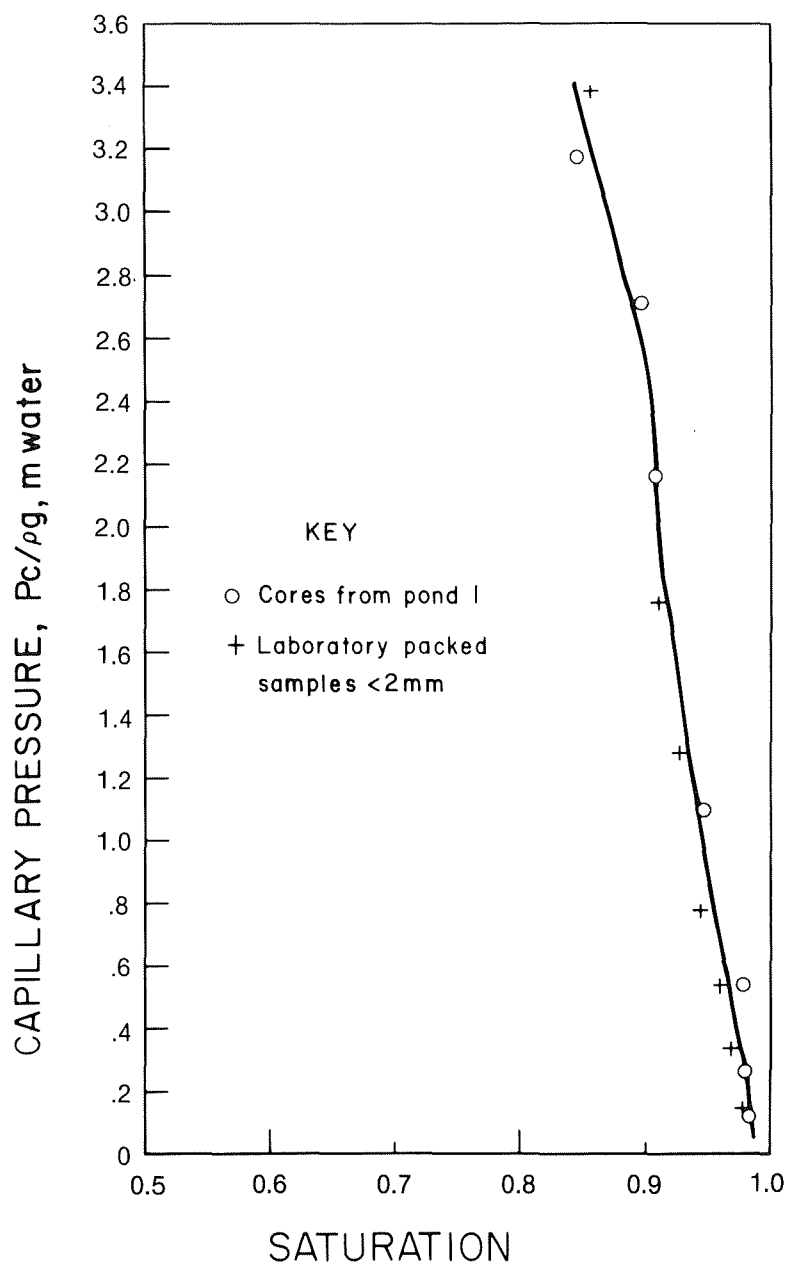


FIGURE 6. - Comparison of capillary pressure-saturation data from undisturbed cores and from laboratory-packed samples.

material is moistened, compacted, and cured. Previous work indicated the natural strength developed is dependent on retorting conditions and that the predominant cementing mechanism is chemical and not mechanical (that is, due to compaction). The specific goals of the Bureau of Mines' funded research project on natural cementation (4) were to--

data used as input to the computer program were obtained from the seepage ponds constructed by Holtz (5). The capillary pressure, saturation, and relative conductivity data used were obtained from undisturbed cores taken from the seepage ponds and from grab samples packed in the laboratory.

The capillary pressure-saturation relationship is shown in figure 6. These data are determined by applying a capillary pressure to each sample and measuring the change in weight by obtaining the change in saturation. Figure 7 presents the relationship between relative conductivity and capillary pressure. This is determined by applying a capillary pressure and then measuring the hydraulic conductivity or permeability. Results of the computer simulation seepage flow compared with actual seepage from ponds are found in the Seepage Ponds section of this report.

#### NATURAL CEMENTATION PROPERTIES

Early in the investigation of material properties of retorted oil shale (5, 7), researchers found indications of an inherent cementation strength when the

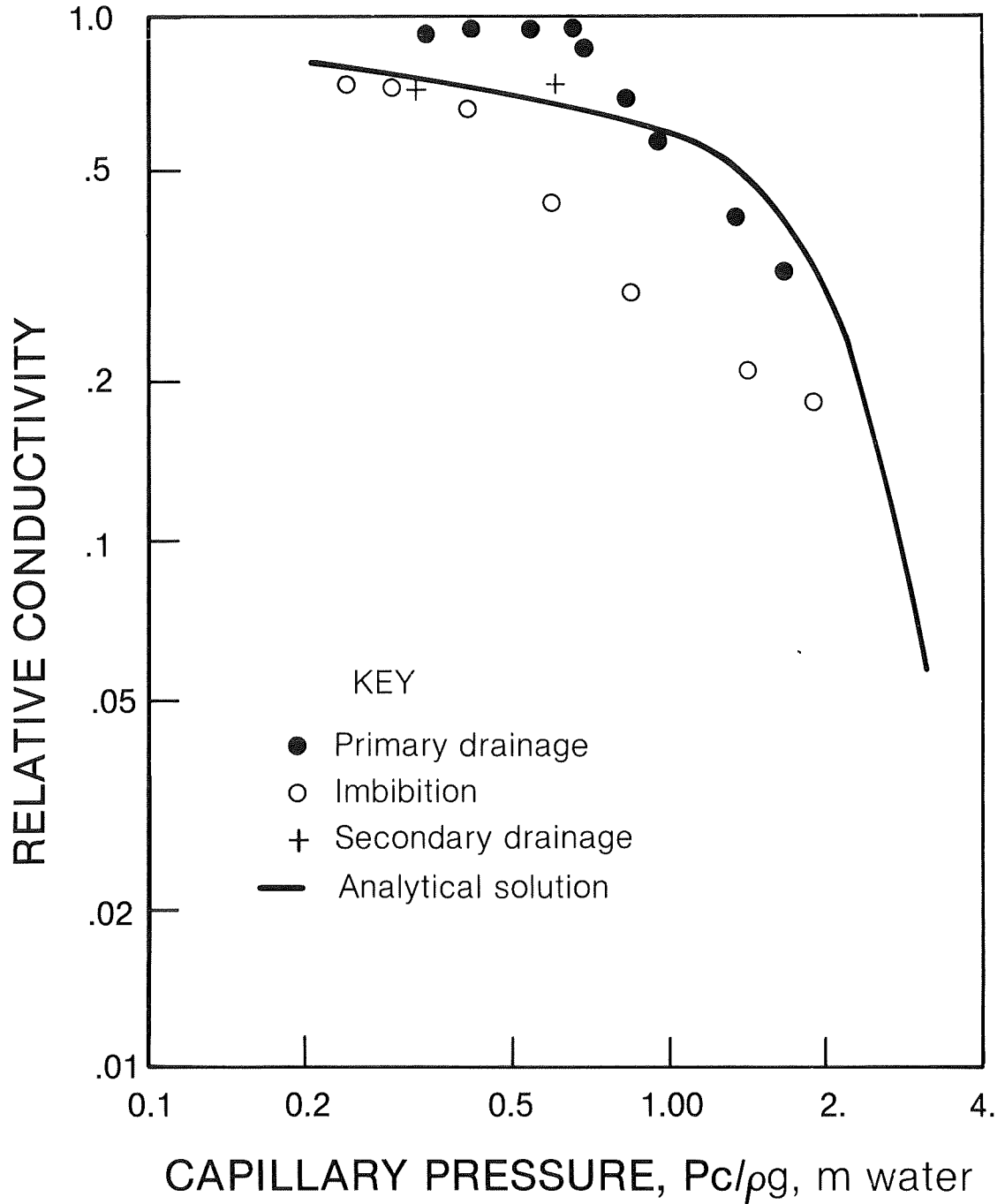


FIGURE 7. - Relative conductivity-capillary pressure curves from undisturbed cores of Paraho compacted retorted oil shale.

1. Optimize natural cementation strength as a function of known and measured retorting variables. Correlate strength as a function of retorting conditions and curing time.

2. Determine the cementing constituent(s) by use of mineralogical and chemical examination.

3. Measure permeabilities and leachate compositions as a function of retort conditions.

4. Determine the effect of retort water on compressive strength and leachate quality, compared with the effect of tapwater.

To meet these goals, the Colorado School of Mine Research Institute's (CSMRI) differential oil shale retort was used. Temperatures and retort residence times ranged between 900 and 1,800° F and 0 to 8 hours, respectively. Other variables investigated were the shale grade, 18 to 33 gal/ton (75 to 138 l/t), and mode of retorting. The mode of retorting refers to the mechanism of heating the shale bed. A direct mode implies the heating of the bed by combustion of residual carbon on the retorted shale within the bed itself; flow of a gas stream containing oxygen through the hot shale bed is necessary. Indirect retorting implies external heating of an inert gas stream prior to its introduction into the retort, where it then heats the bed. Retorting conditions and material were to match as closely as possible to commercial practices. Table 4 shows a comparison of estimated commercial retorting and material conditions to conditions using the CSMRI differential retort.

TABLE 4. - Simulation of commercial retorting conditions

	<u>Estimated commercial practice</u>	<u>CSMRI differ- ential retort</u>
Shale size:		
Inches.....	3/8-3	0-1/2
Centimeters.....	1-7.6	0-1.3
Heating rate:		
° F per hour.....	340-513	1,000-1,300
° C per hour.....	189-285	556-722
Shale grade:		
Gallons per ton.....	25-35	18-33
Liters per ton.....	81-113	55-109
Gas flow:		
Cubic feet per square foot per minute..	3-42	2
Cubic meters per square meter per minute	1-17	0.8
Residence time at temperature, hours.....	2-4	0-8
Gas composition:		
CO <sub>2</sub> , pct.....	° 5-25	0-10
O <sub>2</sub> , pct.....	° 1-10	1-27
Maximum temperature:		
° F.....	900-2,000	900-1,800
° C.....	482-1,093	482-982
Proctor compaction effort:		
Foot-pounds per cubic foot.....	12,375	12,375
Kilogram-meters per cubic meter.....	60,430	60,430
Approach to Proctor density, pct.....	95-100	95-100
Curing temperature of compacted shale:		
° F.....	Ambient	100
° C.....	Ambient	38
<u>Curing time for compacted shale, days....</u>	0-14, 14-indefinite	7-40

° Estimated.

An increase in unconfined compressive strength due to natural cementation was found as temperatures and retort residence time approached optimum. For the direct mode of retorting a maximum of 270 psi (19 kg/cm<sup>2</sup>), compressive strength was obtained at an optimum retorting temperature of 1,510° F (822° C) and residence time of 2.0 hours. For the indirect mode of retorting, a maximum of 325 psi (22.8 kg/cm<sup>2</sup>) was obtained at optimum conditions of 1,530° F (832° C) and 2.9 hours' retort residence time. The material at maximum strength was cured for 28 days at 100° F, had a maximum particle size of 0.5 inch (0.127 cm) with 25 pct moisture content, and was compacted according to ASTM D-698. To maintain strengths above 250 psi, the range of permissible retorting conditions were found to be--

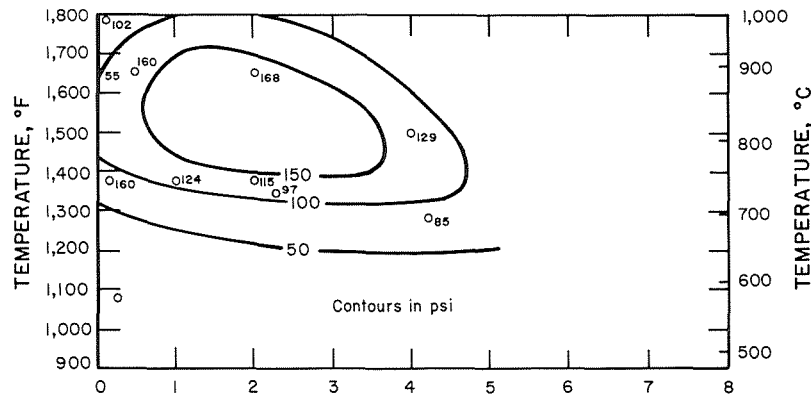
	Direct	Indirect
Retorting temperature.....° F..	1,350-1,700	1,475-1,750
Retorting temperature.....° C..	732-927	803-954
Residence time.....hours..	0.5-3.5	0.5-6.5

In all tests, the strengths increased between 100 and 200 psi as the retorting temperature approached optimum. Figures 8-11 are strength contours at 7, 15, 28, and 40 days' curing time.

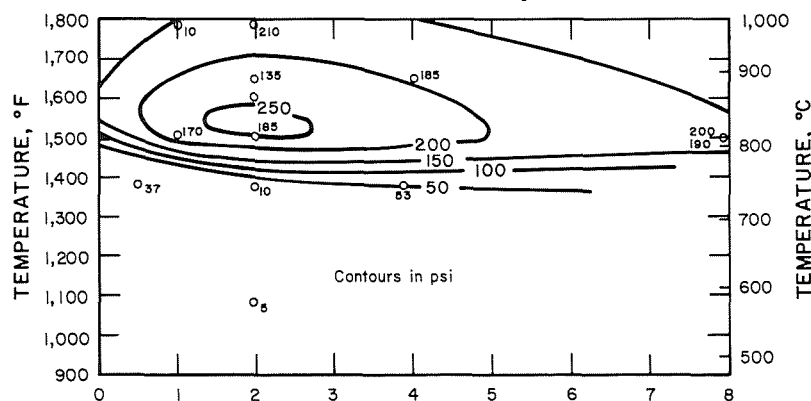
For 14 retort runs, separate density, moisture content, and permeability tests were conducted. The high-temperature retort runs resulted in higher optimum moisture contents and lower maximum densities than previously reported (5) for both retorting modes. Permeabilities were at the high end of the range of 390 to 1,243 ft/yr. These higher permeabilities and lower densities resulted from using a narrower size range of retorted shale, generally higher retorting temperatures, zero applied loading pressure, and a lack of curing of all permeability samples.

Leaching tests on crushed material from the high-strength test cylinders were conducted to determine the changes in leachate quality related to retort residence time, retort temperature, and the use of retort water rather than tapwater during compaction. Carbonates, hydroxides, and aluminum increased at retorting temperature above 1,400° F. Silica slightly increased with increased residence time. Alkalinity dropped with increased residence time. Alkalinity dropped with increased residence time. The pH is directly related to temperature, rising from 9.1 at 1,000° F to 11.3 at 1,400° F (indirect heating mode). Other inorganic constituents in the permeate such as bicarbonate, sulfate, calcium, sodium chloride, and potassium showed no trend relating to compressive strength or retorting conditions. The use of retort water instead of tapwater to moisten the shale before compaction showed no negative impact on the compressive strength. A lower leachate quality was observed; however, it was a relatively small change considering the retort water contained 83 times the level of carbonate, 15 times the sulfate, and 2.5 times the total dissolved solids than the tapwater used.

Samples for the mineralogical analysis were selected from retort runs as typical as possible. High-strength (200-psi) and low-strength (10-psi) cylinders were selected. A raw shale sample was analyzed for a base case. Optical scanning electron microscopy (SEM) and X-ray diffraction were the techniques

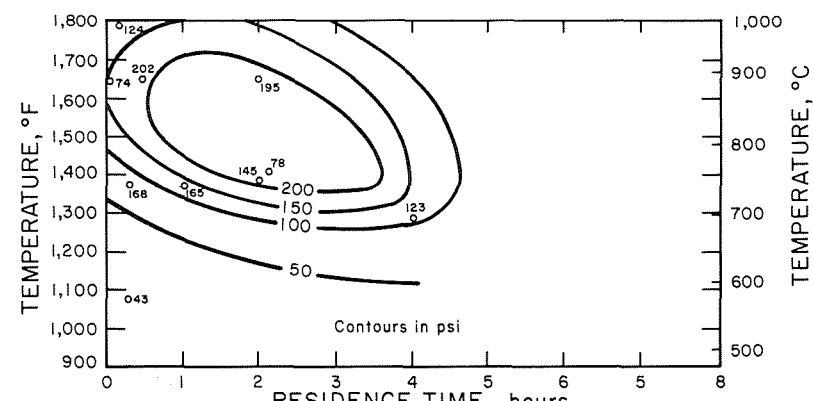


A. Direct mode retorting

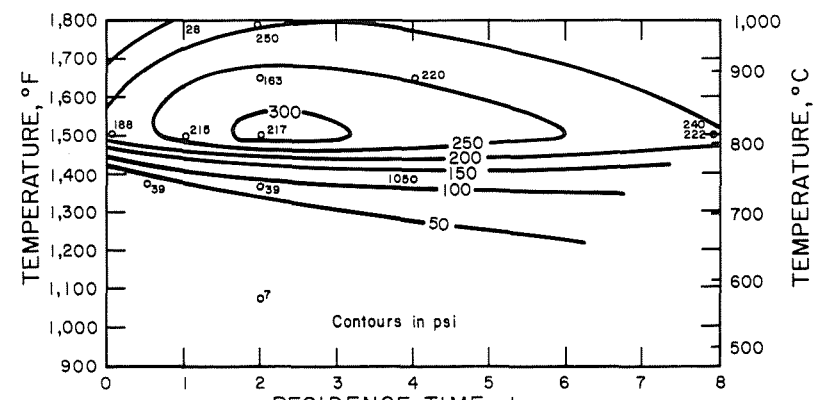


B. Indirect mode retorting

FIGURE 8. - Seven-day compressive strength of retorted oil shale after addition of moisture, compaction, and curing at 100° F.



A. Direct mode retorting



B. Indirect mode retorting

FIGURE 9. - Fifteen-day compressive strength of retorted oil shale after addition of moisture, compaction, and curing at 100° F.

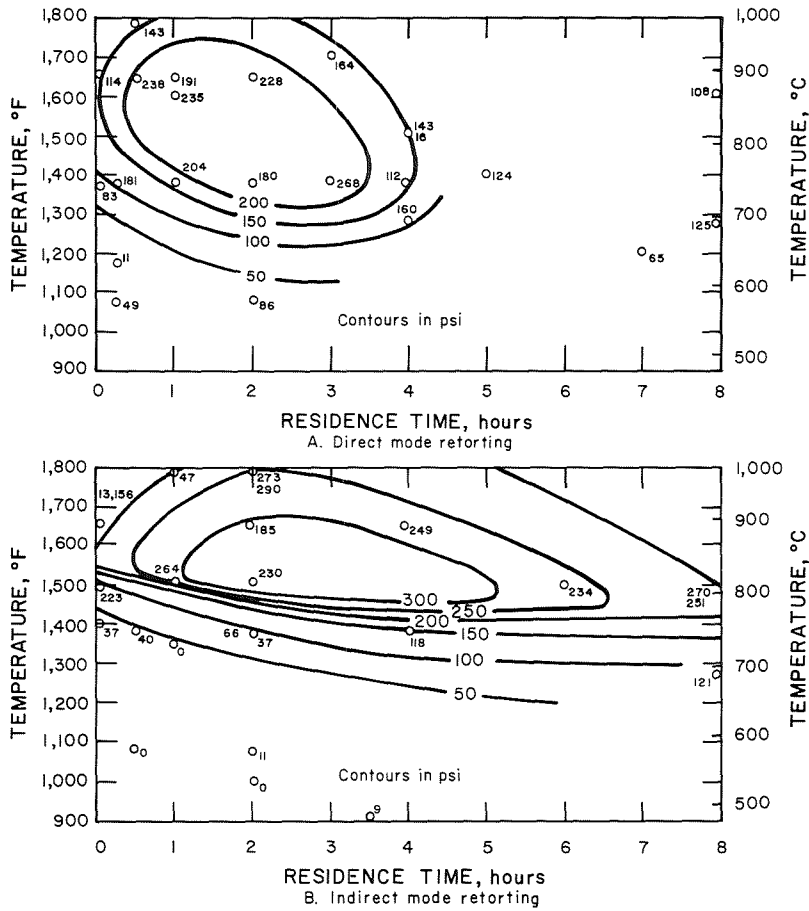


FIGURE 10. - Twenty-eight-day compressive strength of retorted oil shale after addition of moisture, compaction, and curing at 100° F.

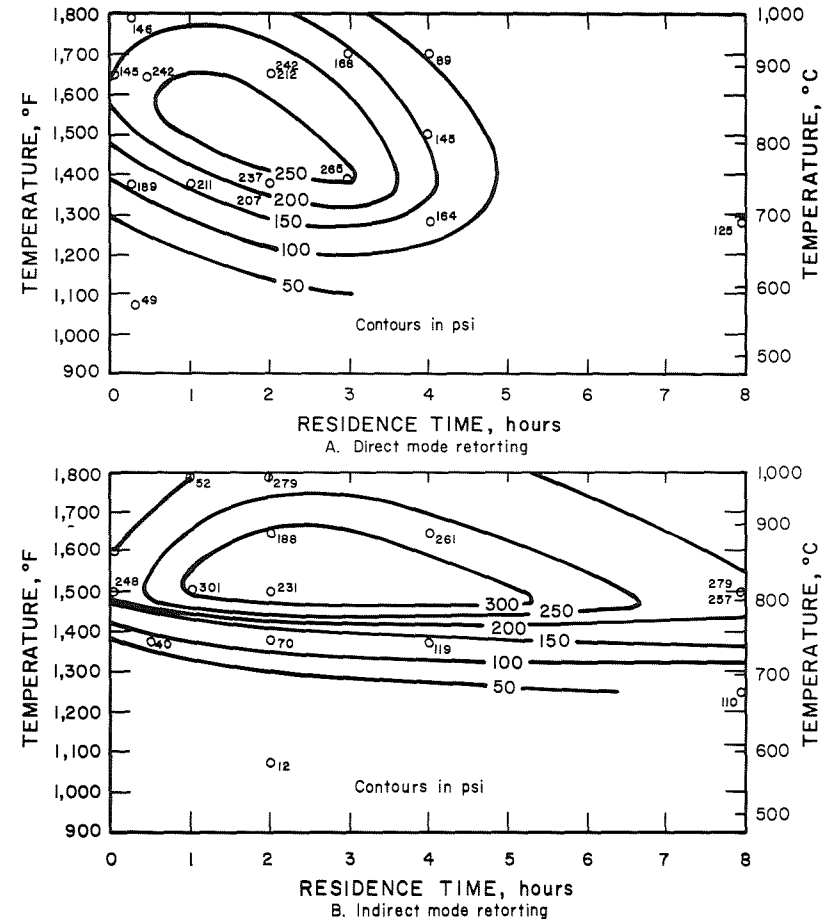


FIGURE 11. - Forty-day compressive strength of retorted oil shale after addition of moisture, compaction, and curing at 100° F.

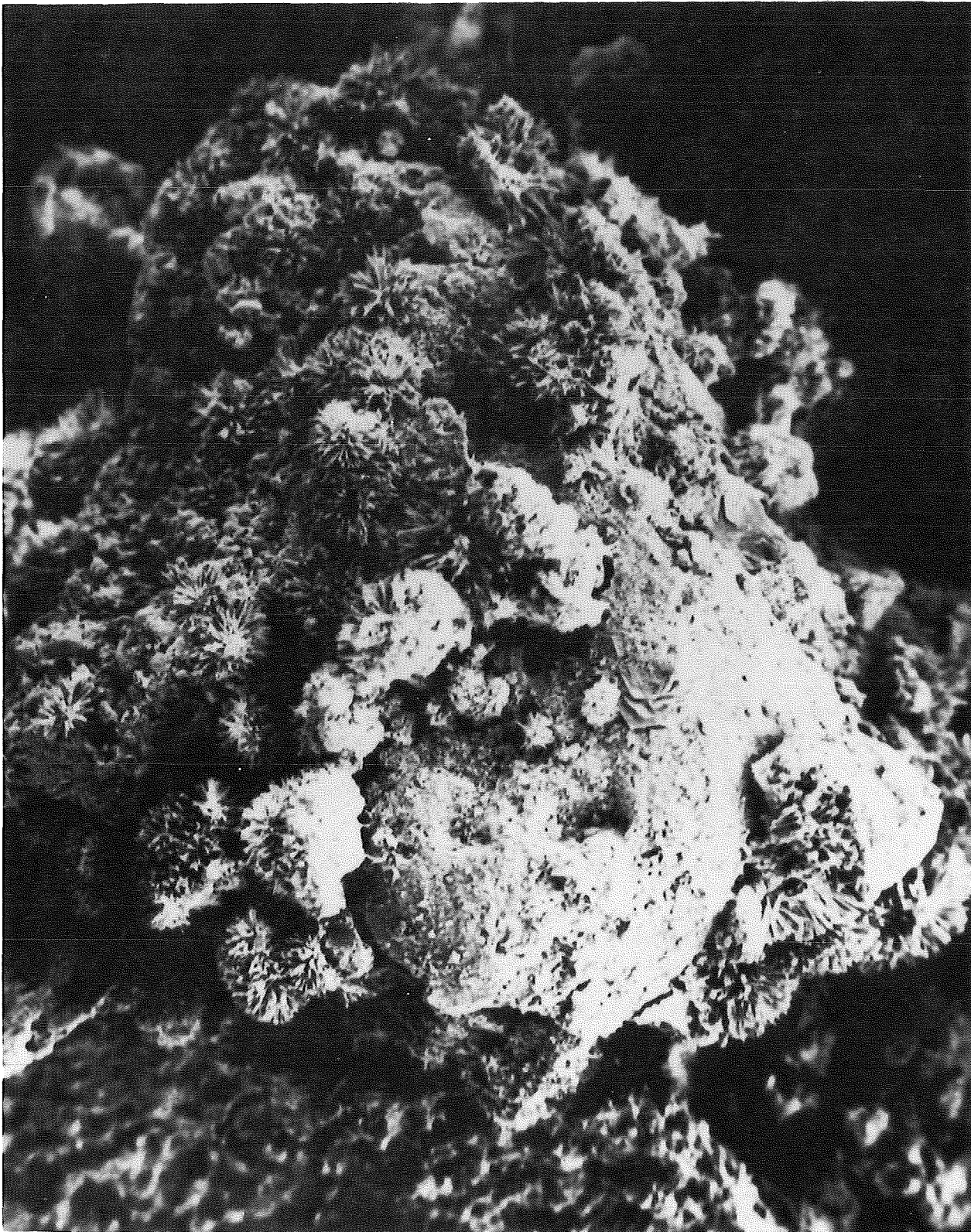


FIGURE 12. - Retorted oil shale fragment with clumps of crystals (X 115).

used for the mineralogical analysis. Using the SEM, typical high-strength samples showed clumps of small interlocking crystals (fig. 12). X-ray fluorescence spectra from these crystals showed peaks of calcium, aluminum, and sulfate. The cementation mechanism appears to be the growth of these crystals at the points of contact between shale fragments. Their span of interlocking effect is up to 50  $\mu\text{m}$  ( $10^{-6}$  m), indicating that the presence of fine shale debris available to form "bridges" between the larger fragment is very important.

#### FIELD TESTS AND MODELING

A field compaction test area and two seepage ponds were constructed of Paraho spent shale and described by Holtz (5). The experiments were conducted at what is now the U.S. Department of Energy, Anvil Points tests site being operated by Development Engineering Inc. Finite-element modeling of the seepage ponds was conducted at the University of Idaho (2).

##### Compaction Tests

The purpose of the field compaction tests was to develop compaction criteria of oil shale that had been retorted in the direct heat mode of the semi-works plant at Anvil Points. The data that was collected included (1) the density that could be achieved by different compaction equipment with different numbers of equipment passes on layers of different thicknesses, (2) particle breakdown under various compaction conditions, (3) density effect of adding water to the fill material, and (4) comparison of the full-scale field compactions with compaction tests in the laboratory in which various degrees of compactive efforts were used. Numerous tests were performed, including in-place density, laboratory standard compaction (ASTM D-698), and laboratory gradation tests on the materials secured from the field test fills before and after compaction. Table 5 summarizes the test fill compaction data, including the percentage of laboratory ASTM D-698 compaction obtained in the field compaction tests.

The test fill was approximately 400 feet (122 m) long by 180 feet (54.9 m) wide, and the completed fill was about 9 feet (2.74 m) thick. Drainage provisions for natural runoff and for seepage or runoff from the test fill were made using culverts, ditches, and a lined evaporation pond. The test fill consisted of two main sections--one section for the placement of material wetted to about optimum moisture prior to compaction, and the other section for placement of material received from the plant in a dry condition with no added moisture.

TABLE 5. - Summary of test fill compaction data

Compaction	Density, pcf				Pct of D-698 compaction			
	Wetted shale		Nonwetted shale		Wetted shale		Nonwetted shale	
	8-inch layers	12-inch layers	8-inch layers	12-inch layers	8-inch layers	12-inch layers	8-inch layers	12-inch layers
Sheep's-foot:								
6 passes.....	91.2	83.7	94.5	89.1	98	88	98	97
10 passes.....	89.6	96.1	94.6	89.8	94	91	97	98
14 passes.....	96.1	81.2	91.7	88.1	102	92	96	96
Pneumatic rubber roller:								
6 passes.....	95.7	89.6	96.7	84.1	99	95	98	92
10 passes.....	91.5	87.6	98.1	92.4	97	94	99	98
14 passes.....	92.8	87.9	101.6	94.4	102	97	102	98
Sheep's-foot, 4 passes, and pneumatic rubber roller,								
6 passes.....	96.6	Nap	Nap	Nap	108	Nap	Nap	Nap
Vibratory pad <sup>1</sup> .....	97.8 (5)	93.9 (12)	<sup>2</sup> 92.2 (6)	<sup>2</sup> 91.7 (6)	104 (5)	104 (12)	<sup>2</sup> 98 (6)	<sup>2</sup> 95 (6)
Vibratory smooth <sup>1</sup> ....	99.7 (6)	100.4 (12)	101.4 (6)	90.7 (9)	110 (6)	110 (12)	104 (6)	98 (9)
Vibratory pad and smooth, 4 passes each.....	99.5	Nap	Nap	Nap	108	Nap	Nap	Nap
Tractor coverages (6)	97.4	Nap	94.2	Nap	102	Nap	102	Nap
Tractor coverages (10)	Nap	Nap	92.3	93.3	Nap	Nap	100	97
Average, all panels.....	93.0		93.1		100		98	

Nap Not applicable.

<sup>1</sup>Numbers in parentheses indicate number of passes.

<sup>2</sup>Final layers not placed.

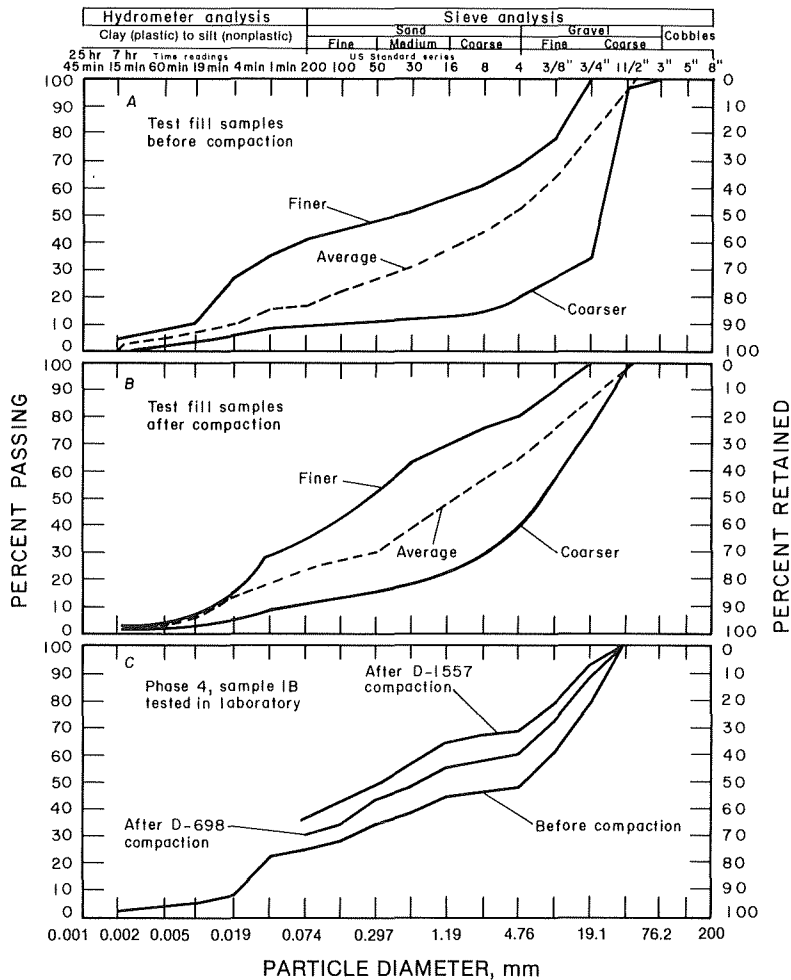


FIGURE 13. - Gradation curves of fill material before and after compaction and of material directly from the retort.

The retorted shale exited from the semiworks plant retort at about 400° F and was hauled to the compaction test site by truck. Approximately 14,000 cubic yards (10,704 m<sup>3</sup>) of shale fill were placed and compacted. The maximum particle size of material placed in the test fill varied from 1-1/2 inches (3.8 cm) to 2-1/2 inches (6.35 cm). The range of gradations and average gradation for material hauled and spread on the fill before (A) and after (B) compaction are shown in figure 13. Also shown (C) is the gradation of material taken directly from the plant (sample 1B) and tested in the laboratory. These figures show that there is about 6 pct less gravel-size material before compaction, as a result of handling, trucking, dumping, and spreading the material. There is an additional 10-pct average loss of gravel-size material resulting from the compaction operations. This results in increases in both the sand and silt sizes.

The compaction equipment used for field tests were (1) a 49,700-pound sheep's-foot roller meeting U.S. Bureau of Reclamation specifications, (2) a 51,700-pound rubber-tired roller, U.S. Engineering Department, Corps of Engineers, (3) a 14,340-pound model 320-A Ray Go<sup>4</sup> vibratory pad type roller, (4) a 20,000-pound model 400-A Ray Go vibratory smooth-drum roller, (5) combinations of 1 through 4, and (6) a D8 Caterpillar tractor.

The results, although not totally consistent, indicate that slightly better compaction was obtained by the heavy rubber-tired roller than by the heavy sheep's-foot roller. The vibratory pad-type roller produced slightly better compaction than either the heavy sheep's-foot or heavy rubber-tired roller. The heavy vibratory smooth-drum roller produced the highest degrees of

<sup>4</sup>Reference to specific equipment, trade names, or manufacturers does not imply endorsement by the Bureau of Mines.

compaction (8- and 12-inch layers), averaging about 105 pct of laboratory D-698 compaction. The results of using the heavy D8 tractor were also good; degree of compaction averaged about 100 pct of laboratory D-698 densities.

Two combinations of compaction equipment were also tested. The combination of the vibratory pad-drum roller and the vibratory smooth-drum roller produced a degree of compaction of 108 percent of laboratory D-698. This is only slightly higher (3 pct) than the compaction produced by the vibratory smooth-drum roller alone. The combination of the sheep's-foot roller and the rubber-tired roller also produced a degree of compaction of 100 pct of laboratory D-698. This combination produced a higher degree (about 9 pct) of compaction than what was achieved by compaction with either one individually.

For all the equipment used, the compaction obtained with comparable number of passes was considerably less for 12-inch (30.48-cm) loose layers than for 8-inch (20.32-cm) loose layers. Six to seven additional passes with the vibratory rollers were required to obtain the same compaction with 12-inch layers as obtained with 8-inch layers. For construction purposes, when high densities are required, 8-inch loose layers (6-inch compacted layers), or less, should be used. The number of equipment passes is also important during compaction, as they can add considerably to the compaction costs. As can be seen in table 5, some unexpected results were obtained. For instance, 10 passes of the sheep's-foot roller produced a lower density than 6 passes (8-inch layer). According to Holtz (5), these variations are caused by changes in the richness, structure, and density of the raw shale; changes in the feed as it passes through the retort; and changes in the operation of the retort. The optimum number of passes should be determined early in the construction phase once the feed and retort operations are stabilized.

For the oil shale retorted in the semiworks plant at Anvil Points, only small differences (an average of 2 pct) in the degree of compaction for wetted and nonwetted material were seen. An average density of 93.0 pcf, or 100 pct of laboratory D-698 compaction, was obtained on the material compacted at optimum moisture. The average density of the shale compacted dry was 93.1 pcf, or 98-pct compaction. This indicates that retorted shale can be compacted to high densities at optimum moisture content or in a dry state. Holtz (5) states, however, that when retorted shale is used for embankment construction material, valley lining, or water-retaining structures, the optimum moisture content of 20 to 22 pct in the material would be necessary to develop low permeability and provide strength gains from cementing properties.

The gradation of materials received for the field compaction tests varied considerably because of operational changes in the semiworks retort, different handling procedures, and different raw shale feed. These conditions varied the particle breakdown characteristics and, in turn, affected the compaction characteristics. These changes made it difficult to obtain reproducible materials for comparing test fill compaction results and laboratory densities. However, the field density data obtained are reasonable and within the range of densities that would be expected in a commercial operation using similar retorting methods.

### Seepage Ponds

Two seepage ponds were constructed of Paraho retorted shale to investigate field permeability values. The two types of permeability data desired were for cases of a moistened, highly compacted fill similar to an impervious section of an earth dam, and for a loosely placed, lightly compacted fill similar to what would be expected to be placed behind a compacted embankment making up the bulk of a disposal site. The construction and measurement details are presented by Holtz (5).

In constructing each pond, a drain pipe was laid in the subgrade with a riser pipe brought up through a 20-mil-thick Hypalon type liner and sealed around the liner. An 8-inch (20-cm) layer of washed gravel was placed over the liner, which allowed any seepage from the shale to drain to the riser pipe and subsequently collect at the outlet.

For pond 1, which would receive the compacted shale lining, an extra layer of loose retorted shale approximately 6 inches (15 cm) thick was placed over the gravel filter layer to further protect the membrane against puncture when the first layer of retorted shale was compacted. It was required that the compacted lining be built up in seven horizontal layers approximately 6 inches (15 cm) thick after compaction to a depth of 3.5 feet (1.1 m). After the bottom lining was completed, the side lining was also constructed in 6-inch (15-cm) compacted horizontal layers in the form of horizontal berms approximately 10 feet (3.1 m) wide. The partially compacted fluff on the southside slope of the lining was then removed for a horizontal distance of about 2.2 feet (0.67 m) to form a compacted lining of 3.5-foot (1.1-m) normal thickness.

The bottom area of pond 1 was 3,010 ft<sup>2</sup> (279 m<sup>2</sup>). The average density based on 18 in-place density tests was 100.6 pcf. This was achieved by seven passes of a Ray Go smooth-drum vibratory roller over each layer of shale. The pond was filled with water to a depth of 3.5 feet (1.1 m), and the computed permeability over a 12-week period was  $4.24 \times 10^{-6}$  cm/sec.

For pond 2, the layers of retorted shale were placed directly on the gravel filter. This pond was built up to a depth of 4 feet in 8-inch (20-cm) loose layers compacted only by the best routing of the truck, front-end loader, and grader during construction. The bottom area was 2,017 ft<sup>2</sup> (187 m<sup>2</sup>). The average dry density of this area was 93.0 pcf.

Two types of permeability tests were run on pond 2. The first was to determine the steady-state seepage rate, which averaged about  $2 \times 10^{-3}$  cm/sec. Several months later the pond was sprinkled with 4,600 gallons (17,400 l) of water to represent a rainfall of 2 inches (5.1 cm) in 30 minutes. Since the pond had partially dried, most of this water was absorbed by the shale and only 1.85 gallons (7.0 l) seeped through the material.

A partially saturated finite-element seepage program developed by Neuman (6) was used to model the seepage from these ponds. The model simulations are described in detail by Bloomsburg (2).

A wide range of time-dependent boundary conditions can be treated: prescribed pressure head, prescribed flux normal to the boundary, seepage faces, and evaporation and infiltration boundaries where the maximum rate of flux is prescribed by atmospheric or other external conditions; whereas the actual rate is initially unknown. A RESTART feature is included in the program, which allows boundary conditions to be changed at any stage of the computation.

The boundary conditions encountered in modeling pond 2 are shown in table 6. Figure 14 shows the comparison of field-measured and simulated flows into the pond. The agreement between simulation and field data is excellent, except after 265 hours when the measured flow was less than predicted. Thus, during the periods between 30 and 150 hours and between 180 and 270 hours when the outlet valve was closed, there is still water moving into the shale increasing the degree of saturation. This particular flow situation cannot be simulated with a conventional saturated flow analysis.

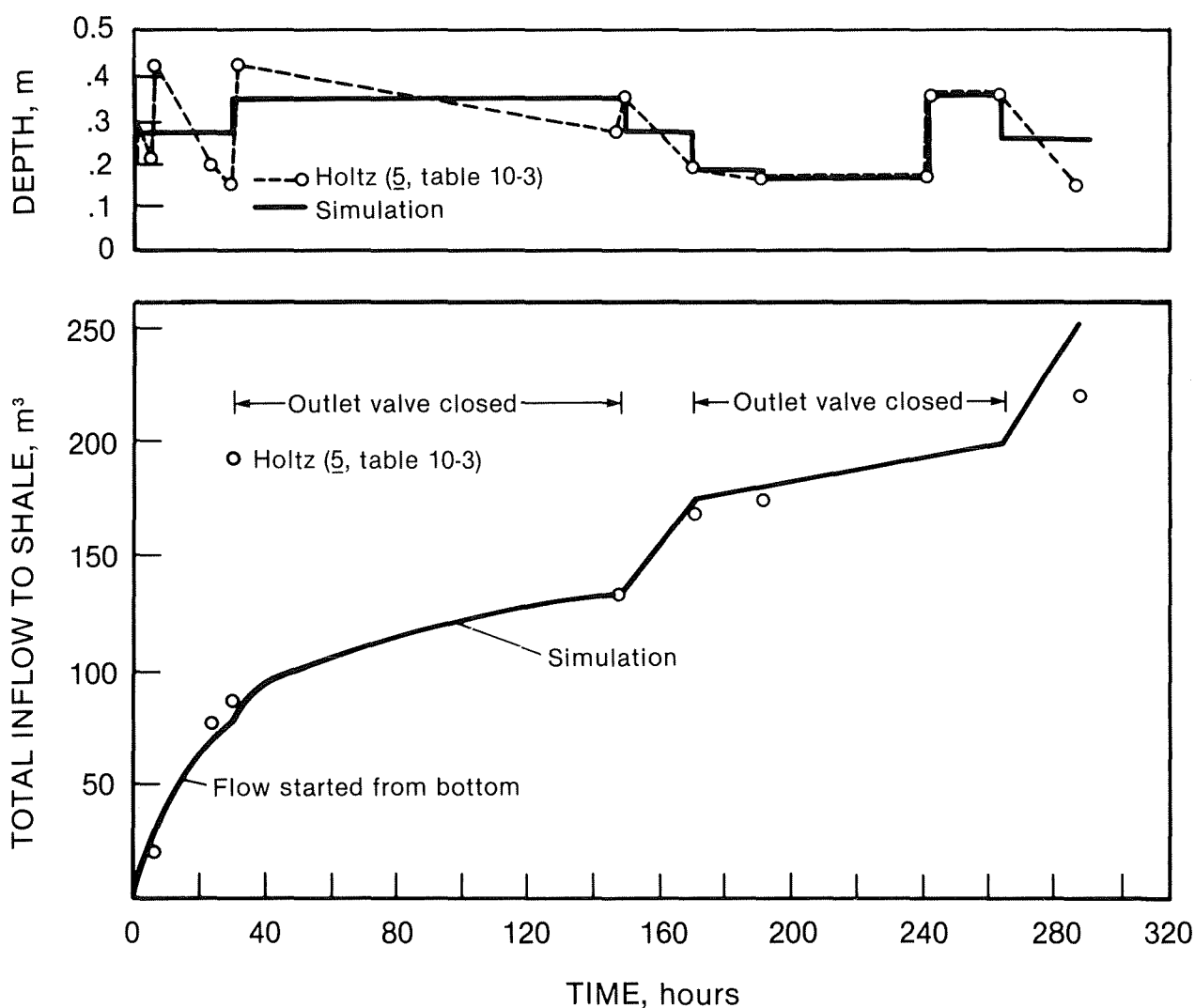


FIGURE 14. - Comparison of actual and simulated flow of water through pond 2 constructed of loose-packed Paraho retorted oil shale.

TABLE 6. - Boundary conditions and values of parameters  
for simulation of pond 2

Date	$\Delta T$ , hours	Top boundary condition (height), m	Bottom boundary condition	Conductivity used, m/yr	Porosity
BEGINNING DATE, DEC. 10					
Dec. 11..	30	0.277	Seepage surface.....	37.9	0.412
Dec. 16..	120	.357	No flow.....	44.8	.453
Dec. 17..	21	.282	Seepage surface.....	52.9	.453
Dec. 18..	50	.183	No flow.....	60.6	.453
Dec. 20..	50	.171	.....do.....	60.6	.453
Dec. 21..	21	.366	.....do.....	60.6	.453
Dec. 22..	24	.259	Seepage surface.....	68.0	.453
BEGINNING DATE, MAY 11					
May 19...	196	0.817	No flow.....	200	0.453
May 19...	7	.817	Seepage surface.....	200	.453
May 20...	7	.488	.....do.....	200	.453
May 20...	6	.223	.....do.....	200	.453
BEGINNING DATE, JUNE 8					
June 15..	170	0.924	No flow.....	200	0.453
June 15..	6	.677	Seepage surface.....	200	.453
June 16..	16	.283	.....do.....	200	.453
June 16..	8.5	.030	.....do.....	200	.453
June 26..	961	( <sup>1</sup> )	.....do.....	200	.453
Nov. 4...	2,424	( <sup>2</sup> )	No flow.....	200	.453
Nov. 6...	95	( <sup>3</sup> )	Seepage surface.....	200	.453

<sup>1</sup>No flow.

<sup>2</sup>Evaporation.

<sup>3</sup>Infiltration.

In general, the agreement between simulation and field data was very good. The last test run on this pond was seepage under rainfall conditions. The pond was sprinkled with 4,600 gallons (17,400 l) over a 30-minute period. The pond had not contained water for about 4 months, so the moisture content of the shale was very low. This evaporation period was simulated to estimate the moisture content at the start of the rainfall test. Table 7 shows the values for the cumulative seepage measured in the field and calculated by the simulation. The simulation showed about 10 times less cumulative leach than was measured in the field. Bloomsburg (2) feels the correlation is very close, considering over 4,600 gallons (17,400 l) of water were applied and that the simulation (over a 4-month period) included evaporation, sprinkling, and an estimated initial moisture content. Because of changes in the physical properties of retorted oil shale, additional research in flow through retorted oil shale is warranted to further validate simulated results versus actual field data.

TABLE 7. - Cumulative leaching after sprinkling

Time after rainfall, hours	Cumulative leach, gallons	
	Field data	Simulation
0.0.....	0.00	0.0
.6.....	.01	.0
1.9.....	.02	.0
3.2.....	.02	.18
6.0.....	.04	.18
22.7.....	1.45	.18
30.2.....	1.64	.18
46.7.....	1.82	.18
70.7.....	1.82	.18
94.7.....	1.82	.18

## PRELIMINARY DISPOSAL SYSTEMS

Underground Disposal

Commercial shale oil production, under the most optimistic estimate, could begin about 1986 at a rate of about 18 million barrels per year (50,000 b/d). When raw shale is crushed prior to gas combustion retorting, the volume per unit mass is doubled. About 40 pct of this volume is then lost in retorting, leaving a spent shale that occupies a 20-percent greater volume than the raw shale in place. Assuming an average grade of raw shale to be 28 gal/ton (116.7 l/t) with an in-place density of 129 pcf, the volume per day of spent shale (50,000 b/d production total surface retorting) would be 1,395,348 ft<sup>3</sup> (39,512 m<sup>3</sup>). This is enough retorted shale to cover 3.2 acres of land 10 feet high each day, if disposed on the surface. Underground backfilling can reduce the surface environmental impact of retorted shale disposal by reducing the land area required to 15 to 30 percent of that required for total surface disposal. From 70 to 85 pct of the retorted shale can be placed back in the mine.

Under contract to Cleveland-Cliffs Iron Co., the Bureau of Mines initiated a research project to determine the most desirable system for underground disposal of oil shale retorted by the Paraho process. Two mining methods, sub-level stoping and chamber-pillar, were specified for backfilling. These methods were considered the most likely conventional mining methods to be employed in the deeper oil shale deposits. A deep underground mine in the central part of Piceance Creek Basin of northwestern Colorado with total surface retorting was assumed. Mechanical, hydraulic, and pneumatic methods of transporting and stowing retorted shale underground were studied individually and in combinations of two or three. Operational considerations included cooling, ventilation, hydrology energy requirements, and monitoring. Cost comparisons of total surface disposal and total underground/surface disposal were made. The physical and chemical characteristics of Paraho direct-heated retorted shale that affect underground backfilling were analyzed.

Seventeen combinations of transport and stowing methods were evaluated and ranked in order to select the most promising method for underground disposal of retorted oil shale. A separate analysis for chamber/pillar and for sublevel stoping was made. The analysis and final ranking were based on (1) subjective technical evaluation, (2) objective technical evaluation, (3) capital costs, and (4) operating costs. The final ranking for the 17 combinations of transport and stowing is shown in table 8 for chamber-and-pillar mining and in table 9 for sublevel stoping. (See Earnest (3) for details on ranking method.)

TABLE 8. - Ranking analysis final selection for chamber-and-pillar mining

(RI = relative importance factor)

Stowing	Subjective technical analysis, RI = 6	Objective technical analysis, RI = 3	Capital costs, RI = 3	Operating costs, RI = 1	Total	Final rank	Final position
CONVEYOR TRANSPORT							
Conveyor.....	6.00	3.00	3.00	1.00	13.00	1.00	1
Pneumatic.....	8.66	4.08	5.21	3.11	21.06	1.62	5
Conveyor and pneumatic topfill.....	7.29	3.33	3.51	1.36	15.49	1.19	2
Hydraulic.....	9.12	11.67	15.27	3.48	39.54	3.04	11
Hydraulic and pneumatic topfill.....	9.54	9.75	14.01	3.23	36.53	2.81	9
TRUCK TRANSPORT							
Truck.....	6.08	3.75	6.69	1.75	18.27	1.41	3
Pneumatic.....	8.36	5.04	8.61	3.89	25.90	1.99	7
Truck and pneumatic topfill.....	7.27	4.05	7.36	2.11	20.79	1.60	4
Hydraulic.....	8.74	12.27	17.51	3.85	42.37	3.26	13
Hydraulic and pneumatic topfill.....	9.18	10.32	16.82	3.79	40.11	3.09	12
PNEUMATIC TRANSPORT							
Vertical pipe.....	10.72	4.44	9.29	3.82	28.27	2.17	8
Borehole.....	9.95	4.26	6.60	3.26	24.07	1.85	6
HYDRAULIC TRANSPORT							
Hydraulic.....	10.51	11.07	13.10	2.46	37.14	2.86	10
Hydraulic and pneumatic topfill.....	11.17	10.14	20.10	3.29	44.70	3.44	14
Conveyor.....	10.54	10.56	20.12	3.79	45.01	3.46	15
Conveyor and pneumatic topfill.....	11.09	10.71	20.64	4.15	46.09	3.58	16
Pneumatic.....	11.38	11.49	21.69	5.83	50.39	3.88	17

TABLE 9. - Ranking analysis final selection for sublevel stowing

(RI = relative importance factor)

Stowing	Subjective technical analysis, RI = 6	Objective technical analysis, RI = 3	Capital costs, RI = 3	Operating costs, RI = 1	Total	Final rank	Final position
CONVEYOR TRANSPORT							
Conveyor.....	6.00	3.00	3.00	1.00	13.00	1.00	1
Pneumatic.....	8.14	3.60	4.59	3.05	19.47	1.50	5
Conveyor and pneumatic topfill.....	7.16	3.33	3.43	1.35	15.27	1.17	2
Hydraulic.....	8.61	11.19	13.45	3.41	36.66	2.82	11
Hydraulic and pneumatic topfill.....	8.95	9.24	12.35	3.17	33.71	2.59	9
TRUCK TRANSPORT							
Truck.....	6.20	3.75	6.14	1.69	17.78	1.37	3
Pneumatic.....	7.92	4.71	7.58	3.81	24.02	1.85	7
Truck and pneumatic topfill.....	7.11	4.02	5.99	2.03	19.15	1.47	4
Hydraulic.....	8.23	11.79	15.42	3.77	39.21	3.02	13
Hydraulic and pneumatic topfill.....	8.65	9.84	14.82	3.71	37.02	2.85	12
PNEUMATIC TRANSPORT							
Vertical pipe.....	10.16	4.08	8.18	3.75	26.17	2.01	8
Borehole.....	9.34	3.90	5.82	3.20	22.26	1.71	6
HYDRAULIC TRANSPORT							
Hydraulic.....	9.79	10.56	11.54	2.42	34.31	2.64	10
Hydraulic and pneumatic topfill.....	10.39	10.11	17.71	3.23	41.44	3.19	14
Conveyor.....	9.79	10.56	17.73	3.72	41.80	3.22	15
Conveyor and pneumatic topfill.....	10.24	10.71	18.18	4.07	43.20	3.32	16
Pneumatic.....	10.61	11.40	19.11	5.72	46.84	3.60	17

The conveyor transport and stowing methods ranked highest of the 17 methods studied. This method has (1) lowest personnel and energy requirements, (2) lowest capital and operating costs, (3) highest pillar support potential and greatest potential for increased resource recovery, (4) most retorted shale placement underground and highest fill density, (5) least surface disruption, ground-water contamination, and environmental degradation, and (6) safest overall method.

Both hydraulic and pneumatic transport and stowing systems were found to be less favorable. The Paraho retorted shale material degraded excessively when slurried and pumped, reducing the dewatering capability of the fill. The safety factor was less and costs higher for a hydraulic system because of the need for large, reliable bulkheads, high energy, and high water requirements. The pneumatic system had excessive capital and operating costs, with high energy requirements (horsepower per ton). Increased ventilation requirements

would be needed to handle the dust problem. Several blower-feeder units and pipeline networks would be required to attain the necessary transport and stowage.

Total underground and surface retorted shale disposal costs (fourth quarter, 1977 dollars), using conveyor transport and stowing, will be approximately \$0.80 per ton of retorted shale or \$1.10 per barrel of shale oil produced. This is about twice as high as total surface disposal without backfilling. However, backfilling will greatly reduce surface environmental impacts and subsidence, and increased resource recovery of about 15 pct is possible since the stabilizing effect of backfilling permits the use of relatively thin pillars.

Several methods to change the physical properties of retorted oil shale for backfill enhancement were investigated. Compaction of stowed material improves its strength and resistance to saturation by ground water. Also, more material can be stowed if compacted. A mechanical compactor with a blade attachment for spreading is required for adequate compaction. Because of degradation when hydraulically pumped, flocculents and cementing agents did not improve the strength characteristics of the fill material. However, a 5-to-1 retorted shale-cement mixture at 15 pct moisture content produced a large increase in compressive strength after 8 days of curing. Drainage characteristics were tested in the laboratory using vertical perforated pipe and perforated bottom drains. For a slurry containing 34 to 38 wt-pct solids, 71 pct of the water drained using vertical pipe drains and 67 pct of the water drained using perforated bottom drains.

The current trend in oil-shale mining methods is modified in situ retorting. Underground depleted retorts will probably require backfilling to fill the voids of the rubblized material for environmental and support purposes. Conveyor stowage will not be feasible for this method. A current Bureau of Mines contract with Rio Blanco Oil Shale Co. will attempt to develop a slurry filling system for modified in situ retorts, which will minimize surface and underground environmental disturbance. The 20 to 25 pct of shale retorted on the surface will be injected into the in situ shale rubble in a coherent mass sufficiently strong to resist subsidence. The filled, depleted retort will be vertically impermeable and, therefore, minimize contamination of the ground water and its aquifers. Control of retorted shale slurry properties will be a major problem.

#### Surface Disposal

When investigating a hypothetical surface disposal system, both seepage and stability analysis were performed. The overall dimensions of the surface fill, analyzed in figure 15, are 1,880 feet (573 m) horizontally and 300 feet (91 m) vertically. The initial moisture conditions (on dry-weight basis) were 25 pct for the embankment and 20 pct for the fill. The densities were 95 and 85 pcf, respectively. The fill was studied under three seepage boundary conditions:

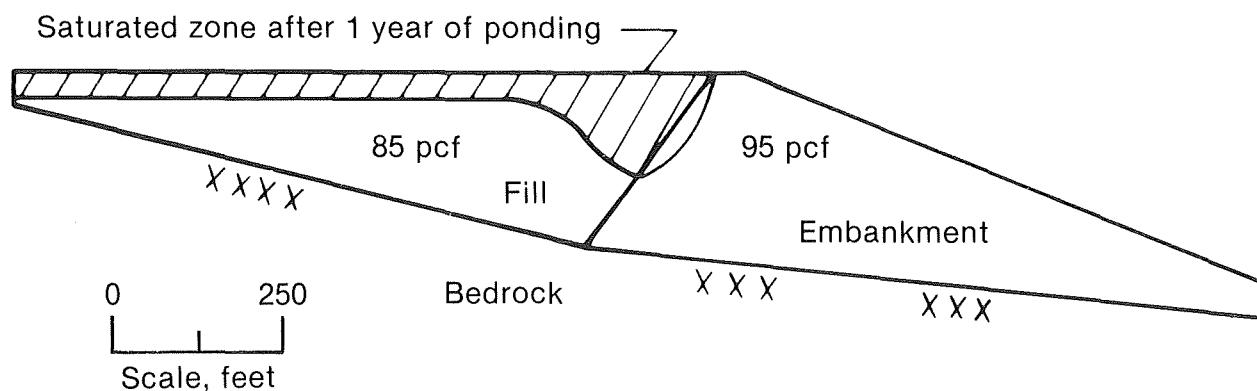


FIGURE 15. - Typical cross-valley fill and simulated saturation zone after 1 year of ponding.

1. A 100-year, 1-hour storm (intensity of 0.95 inch per hour).
2. A 100-year, 6-hour storm (intensity of 0.25 inch per hour).
3. A ponded condition of 5 feet (1.5 m) of water on the surface for a period of 1 year, and no infiltration or evaporation on the remainder of the pile. The 100-year storm data are applicable for northwestern Colorado.

The two storm intensities were selected to determine whether rainfall would infiltrate the waste pile or run off the surface. Results of the two storm simulations were similar. There was no runoff at any time during either storm for the 85-pcf shale. The moisture content in the upper layer increased by about 0.5 pct. This water would be held in the upper layer until evaporated, since it did not seep down into the pile. In both cases there was substantial runoff from the 95-pcf shale (infiltration rate was less than the rainfall rate), and therefore only a slight increase in moisture content was detected. This result indicates a need for berms on the downslope side of the embankment for erosion control, and diversion channels for runoff control. Contamination of surface or ground water from leachate would not appear to be a problem.

In the analysis of the ponded boundary condition, the ponded area extended over the entire surface of the 85-pcf shale. This problem was studied by simulation for a period of 1 year. The regions that became saturated are indicated in figure 15. The saturated zone had moved into the shale as much as 40 feet (12.2 m) from the surface and moved considerably deeper than that at the left end of the 95-pcf shale. With this type of situation, the simulation suggests that the impoundment would become saturated, and protection of surface and ground water would have to be considered.

#### Stability Analysis

Using the Bishop technique, stability analysis was performed on both a dry and worst-case saturated valley fill retorted oil shale waste bank. Densities, cohesion ( $c$ ), and angle of internal friction ( $\phi$ ) found in the laboratory tests were used in the analysis. For the dry condition, densities

were 85 pcf in the fill and 95 pcf in the embankment. Cohesion and  $\phi$  were 3.25 psi and  $33^\circ$ , respectively. For the worst-case saturated condition, densities were 90 pcf in the fill and 100 pcf in the embankment. Cohesion and  $\phi$  were the same as in the dry state. The calculated centers of rotation (dry and wet) and the circular arc failure planes can be seen in figure 16. Factor of safety is 1.673 for the dry state and 0.849 for the wet state. The unstable condition in the wet state indicates that either an impervious core or adequate drainage facilities need to be installed to prevent saturation of the fill with high-phreatic surface conditions.

Holtz (5) found that densities between 95 and 107 pcf were obtained during construction of filtration pond 1. Permeability rates for this pond were 4.24 ft/yr ( $4.2 \times 10^{-6}$  cm/sec). Evaporation rates were not measured, indicating that even a lower permeability or a near impervious condition was obtained. With this in mind, the next step in the stability analysis was to improve the safety factor of a proposed saturated cross-valley spent shale fill. A spent shale core, compacted at 105 pcf, was placed inside the spent shale of the simulated embankment. The embankment material was placed at 95 pcf around the core, and the saturated fill upstream of the embankment was assumed to be

KEY

Soil	$\gamma$ , pcf		c, psi	$\phi$ , degrees
	Dry/Wet			
1	95/100		3.25	33
2	95/100		3.25	33
3	85/90		3.25	33
4	85		3.25	33
5	95		3.25	33

Factor of safety, wet = 0.849  
 Factor of safety, dry = 1.673  
 $\nabla$  = Phreatic surface

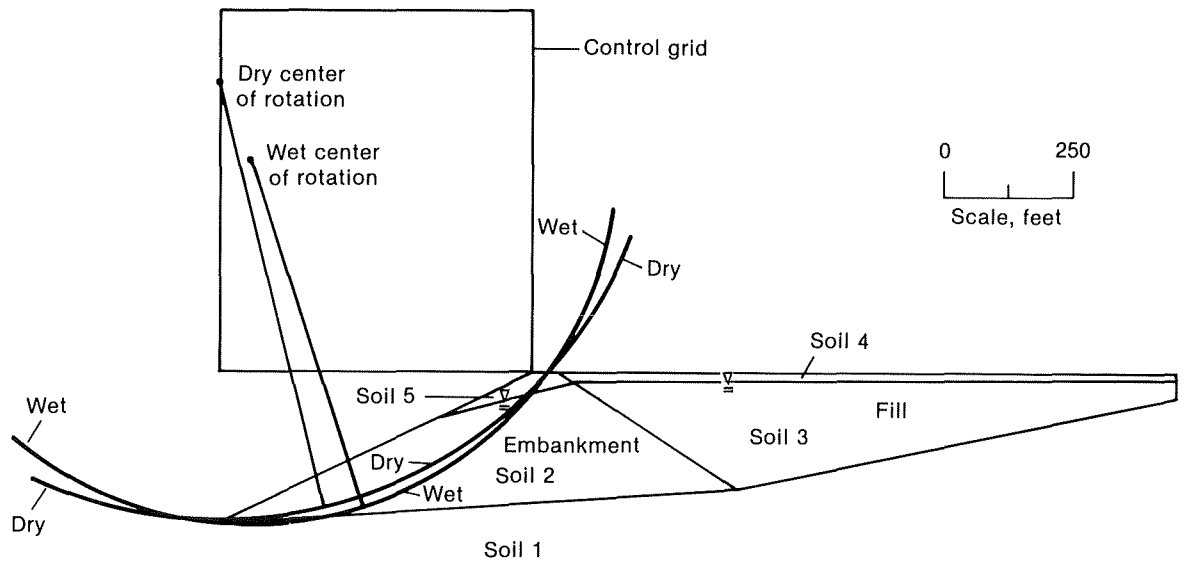


FIGURE 16. - Circular arc failure planes and safety factors for a saturated and dry retorted oil shale fill.

KEY			
Soil	$\gamma$ , pcf	c, psi	$\phi$ , degrees
1	105	3.25	33
2	95	3.25	33
3	85	3.25	33

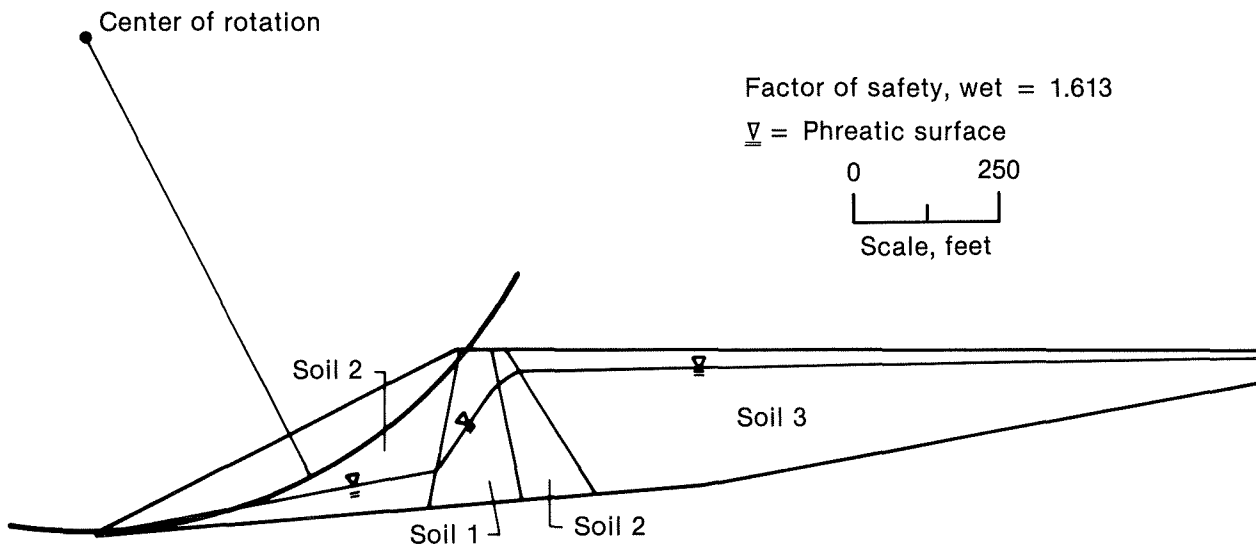


FIGURE 17. - Circular arc failure plane and safety factor for a saturated retorted oil shale fill with a core. Phreatic surface is assumed.

85 pcf. Cohesion and  $\phi$  were the same as in the previous saturated case (3.25 psi and  $33^\circ$ , respectively). Figure 17 shows the center of rotation and circular arc failure plane as determined by the Bishop technique. The factor of safety was calculated to be 1.613 using the assumed phreatic surface shown in the figure. This analysis indicates that under saturated fill conditions, a highly compacted core will improve the safety factor. However, one should never completely assume a phreatic level in analyzing safety factors of planned structures. Graphical solutions (flow nets) derived by hand for simple cases, or by digital computer methods for more complicated cases, should be used. For the anisotropic homogeneous case shown in figure 17, it is quite likely that an inclined (chimney) drain would be required to achieve the phreatic line as was assumed.

### CONCLUSIONS

The data and results presented in this report are intended to summarize a vast amount of information governing several aspects of disposal of spent oil shale. This information will be useful in developing preliminary designs for either research or commercial disposal systems.

Design engineers must keep in mind that the spent shale used in determining the information presented in this report was retorted under changing,

experimental retort conditions. A commercial operation will most likely produce a waste product having somewhat different properties. Changes in retort conditions also produce a slight change in the waste properties.

Therefore, before detailed, large-scale designs are developed, a small series of tests should be run on spent shale retorted under the expected operating conditions. These results should be compared with available data. If discrepancies are apparent, some detailed laboratory testing should be performed to obtain valid engineering properties.

REFERENCES<sup>5</sup>

1. American Society for Testing and Materials. 1974 Annual Book of ASTM Standards. Part 19, Soil and Rock, Building Stones, Peats. Philadelphia, Pa., pp. 70-80, 148-153, 212-217, 252-260, 264-267; 1975 Annual Book of ASTM Standards, Part 14, Concrete and Mineral Aggregates. Philadelphia, Pa., pp. 84-87, 321-322.
2. Bloomsburg, G. L., and R. D. Wells. Seepage Through Partially Saturated Shale Wastes. BuMines Open File Rept. 63-79, September 1978, 155 pp.; available from National Technical Information Service, Springfield, Va., PB 297 300/AS; contract H0252065, University of Idaho.
3. Earnest, H. W., R. A. Heisler, H. L. Hoe, and V. Rajaram. Underground Disposal of Retorted Oil Shale for the Paraho Retorting Process. BuMines Open File Rept. 1-80, May 1978, 379 pp.; available from National Technical Information Service, Springfield, Va., PB 80-128739; contract J0265052, Cleveland-Cliffs Iron Co.
4. Farris, C. B. Natural Cementation of Retorted Oil Shale. BuMines Open File Rept. 54-80, May 1979, 131 pp.; available from National Technical Information Service, Springfield, Va., PB 80-179138; contract J0285001, Colorado School of Mines Research Institute.
5. Holtz, W. G. Disposal of Retorted Oil Shale From the Paraho Oil Shale Project--Final Report. BuMines Open File Rept. 27-77, December 1976, 474 pp.; available from National Technical Information Service, Springfield, Va., PB 263 793/AS; contract J0255004, Development Engineering Inc. and Woodward-Clyde Consultants.
6. Neuman, S. P., R. A. Feddes, and E. Bressler. Finite Element Simulation of Flow in Saturated-Unsaturated Soils Considering Water Uptake by Plants. Israel Inst. of Technology, Haifa, Israel, 3d Ann. Prog. Rept. A10-SWC-77, 1974, 104 pp.
7. Nevans, T. D., C. H. Habenicht, and W. J. Culbertson, Jr. Disposal of Spent Shale Ash in "In-Situ" Retorted Caverns. Denver Res. Inst., Univ. Denver, Colo., May 1977, 64 pp.
8. Silver, M. L., and others. Cyclic Triaxial Strength of Standard Test Sand. J. Geotech. Eng. Div., ASCE, v. 102, No. GT5, 1976, pp. 511-523.

---

<sup>5</sup>Bureau of Mines Open File Reports cited are available for consultation at the Bureau of Mines libraries in Denver, Colo., Twin Cities, Minn., Bruceton and Pittsburgh, Pa., and Spokane, Wash.; U.S. Dept. of Energy facilities at Carbondale, Ill., and Morgantown, W. Va.; the National Mine Health and Safety Academy, Beckley, W. Va.; and the National Library of Natural Resources, U.S. Dept. of the Interior, Washington, D.C.

9. Snethen, D. R., W. J. Farrell, and F. C. Townsend. A Review of the Physical and Engineering Properties of Raw and Retorted Oil Shales From the Green River Formation. U.S. Army Corps of Engineers, Waterways Exp. Sta., Vicksburg, Miss., Rept. WES MP S-78-3, 1978, 40 pp.
10. Townsend, F. C., and R. W. Petersen. Geotechnical Properties of Oil Shale Retorted by the Paraho and Tosco Processes. BuMines contract report, 1979, 271 pp. (to be placed on open file); available from National Technical Information Service, Springfield, Va., pub. WES-A082317/9; BuMines contract H0262064, U.S. Army Corps of Engineers, Waterways Experiment Station.
11. U.S. Army, Corps of Engineers. Laboratory Soils Testing. Eng. Manual 1110-2-1906, 1979.
12. U.S. Bureau of Reclamation. Earth Manual. 2d ed., 1974, pp. 327-642.
13. Wung, R. T., H. B. Seed, and C. K. Chan. Cyclic Loading Liquefaction of Gravelly Soils. J. Geotech. Eng. Div., ASCE, v. 101, No. GT6, 1975, pp. 571-583.

## APPENDIX.--NOMENCLATURE

$A_v$  = Coefficient of compressibility  
 $B$  = Breakage factor  
 $c$  = Cohesion  
 $c'$  = Effective cohesion  
 $C_c$  = Compression index  
 $C_v$  = Coefficient of consolidation  
CD = Consolidated-drained  
CU = Consolidated-undrained  
 $d$  = Dry density  
 $d_r$  = Relative density  
 $e$  = Void ratio  
 $e_o$  = Initial void ratio  
 $\Delta e$  = Change in void ratio  
 $E$  = Vertical strain  
 $g$  = Acceleration due to gravity  
 $H$  = Vertical height  
 $k$  = Permeability  
PPR = Pore pressure response  
 $P_c$  = Capillary pressure  
 $P_1$  = Initial stress  
 $P_2$  =  $P_1$  + change in stress  
 $\Delta P$  = Change in pressure  
RI = Relative importance factor  
 $t$  = Time  
 $\Delta T$  = Time interval  
U/C = Unconfined compression  
 $W$  = Water content

Symbols

$\gamma_w$  = Unit weight of water

$\rho$  = Fluid mass density

$\gamma$  = Density

$\phi$  = Angle of total stress

$\phi'$  = Angle of effective stress

$\sigma_1$  = Major principal stress

$\sigma_{de}$  = Cyclic deviator stress

$\sigma_3$  = Minor principal stress

$\nabla$  = Phreatic surface







